Marine Carbohydrates in Arctic Aerosol Particles and Fog – Diversity of Oceanic Sources and Atmospheric Transformations

Sebastian Zeppenfeld[1], Manuela van Pinxteren[1], Markus Hartmann[2], Moritz Zeising[3], Astrid Bracher[3,4], and Hartmut Herrmann[1]

1 Atmospheric Chemistry Department (ACD), Leibniz-Institute for Tropospheric Research (TROPOS), Leipzig, Germany
2 Atmospheric Microphysics (AMP), Leibniz-Institute for Tropospheric Research (TROPOS), Leipzig, Germany
3 Alfred-Wegener-Institute Helmholtz Centre for Polar and Marine Research, Bremerhaven, Germany
4 Institute of Environmental Physics, University of Bremen, Bremen, Germany

Correspondence to: Hartmut Herrmann (herrmann@tropos.de)

Submitted to Atmospheric Chemistry and Physics 2023

Abstract

Carbohydrates, produced and released by marine microorganisms in the ocean, enter the atmosphere as part of sea spray aerosol (SSA) and can influence fog and cloud microphysics by acting as cloud condensation nuclei (CCN) or ice nucleating particles (INP). Particularly in the remote Arctic region, significant knowledge gaps persist about the sources, the sea-to-air transfer mechanisms, atmospheric concentrations, and processing of this substantial organic group. In this study, we present the results of a ship-based field study conducted from May to July 2017 in the Fram Strait, Barents Sea and central Arctic Ocean about the sea-air transfer of marine combined carbohydrates (CCHO) from concerted measurements of the bulk seawater, the sea surface microlayer (SML), aerosol particles and fog. In seawater, CCHO ranged between 22–1070 µg L^{-1} with large differences among the different sea-ice-related sea surface compartments: ice-free ocean, marginal ice zone (MIZ), open leads/polynyas within the pack ice and melt ponds. Enrichment factors in the SML (EF_{SML}) relative to the bulk water were very variable in the dissolved (0.4–16) and particulate (0.4–49) phases with highest values in the MIZ and aged melt ponds. In the atmosphere, CCHO appeared in super- and submicron aerosol particles ($CCHO_{aer,super}$: 0.07–2.1 ng m^{-3}; $CCHO_{aer,sub}$: 0.26–4.4 ng m^{-3}) and fog water ($CCHO_{fog,liquid}$: 18–22000 µg L^{-1}; $CCHO_{fog,\ atmos}$: 3–4300 ng m^{-3}). The enrichment factors for the sea-air transfer were calculated for super- and submicron aerosol particles and fog, however strongly varied depending on which of the sea-ice-related sea surface compartments were assumed as the oceanic emission source. Finally, we observed a quick atmospheric aging of CCHO after their emission with indications for both

biological/enzymatic processes (based on very selective changes within the monosaccharide compositions of CCHO) and abiotic degradation (based on the depolymerization of long-chained CCHO to short free monosaccharides). All in all, the present study highlights the diversity of marine emission sources in the Arctic Ocean and atmospheric processes influencing the chemical composition of aerosol particles and fog.
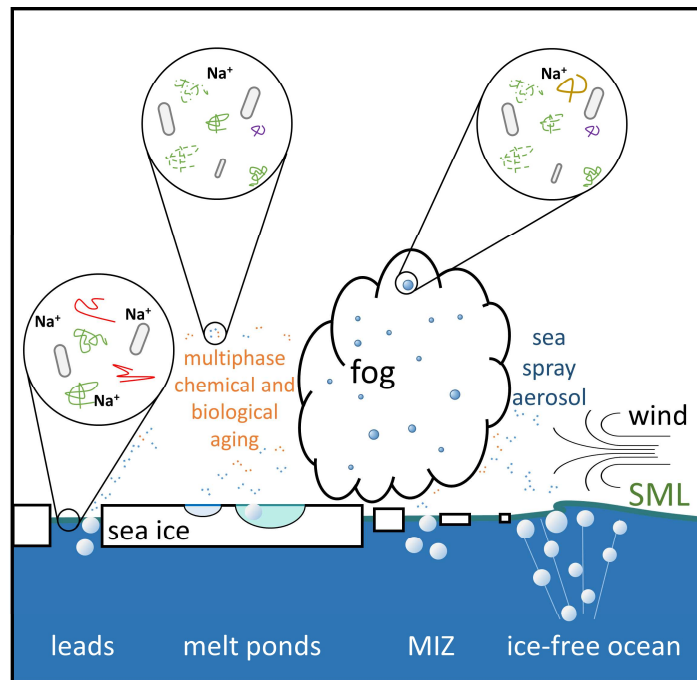
TOC Figure

1. Introduction

Sea spray aerosol (SSA) represents one of the major aerosol species in the lower troposphere over the remote Arctic Ocean, particularly during the spring and summer months in the Northern Hemisphere (Chi et al., 2015; Hara et al., 2003; Kirpes et al., 2018; May et al., 2016). Depending on the size distribution and chemical composition, SSA particles strongly contribute to the populations of cloud condensation nuclei (CCN) and ice nucleating particles (INP) affecting the polar radiative budget through the formation of liquid droplets and ice crystals in fog and clouds (DeMott et al., 2016; Lawler et al., 2021; McCluskey et al., 2018; Penner et al., 2001; Schiffer et al., 2018; Wilbourn et al., 2020). Notably in the Arctic, one of the regions most affected by global warming, there is still a lack of knowledge about the relationship between the formation and evolution of clouds and specific chemical properties of SSA particles (Wendisch et al., 2023).

SSA is emitted directly from the ocean surface through wind-driven processes and, as a consequence, contains the salts and the organic matter (OM) present in seawater, including carbohydrates (CHO) as one of the largest identified organic fractions (Quinn et al., 2015 and references therein). In microalgae, bacteria and also more complex marine organisms (e.g. kelp, krill), carbohydrates have important metabolic, structural and protective functions or are released in response to environmental stress, such as freezing or lack of nutrients (Krembs et al., 2002; Krembs and Deming, 2008; McCarthy et al., 1996; Mühlenbruch et al., 2018; Suzuki and Suzuki, 2013; Wietz et al., 2015). In seawater, most carbohydrates appear as linear or branched oligo- and polysaccharides, commonly referred to as combined carbohydrates (CCHO). They can be found in both dissolved (dCCHO) and particulate (pCCHO) phases, distinguished operationally by a 0.2 µm filtration. These macromolecules consist of several monosaccharides, such as hexoses, pentoses, deoxy sugars, amino sugars, uronic acids and amino sugar acids, which are connected via glycosidic bonds (Benner and Kaiser, 2003; Engel and Händel, 2011; Panagiotopoulos and Sempéré, 2005). Most CCHO are quite stable within the marine environment unless they are either hydrolyzed in the presence of specific enzymes or in a very acidic setting (Arnosti, 2000; Panagiotopoulos and Sempéré, 2005). Heterotrophic bacteria use extracellular enzymes to selectively degrade CCHO into absorbable shorter molecules leaving a certain part as recalcitrant, more persistent OM (Alderkamp et al., 2007; Becker et al., 2020; Goldberg et al., 2011; Wietz et al., 2015). While pCCHO is mostly attributed to recent productions by local phytoplankton indicated by high positive correlations with total chlorophyll a (TChl-a), dCCHO appears to be the result of more complex metabolic and transformation processes after its release (Becker et al., 2020; Fabiano et al., 1993; Goldberg et al., 2011; Zeppenfeld et al., 2021a). In contrast, dissolved free carbohydrates (dFCHO), short sugars in their monomer form, are quickly consumed by marine microorganisms

76 resulting in much lower concentrations of *d*FCHO compared to CCHO in ambient seawater (Engbrodt,

77 2001; Engel and Händel, 2011; Ittekkot et al., 1981; Zeppenfeld et al., 2020).

78 In the remote marine atmosphere, carbohydrates are suggested to significantly impact cloud

79 properties by contributing to both the CCN and INP populations (Alpert et al. 2022; Leck et al., 2013;

80 Orellana et al., 2011; van Pinxteren et al., 2022). Carbohydrates appear both in super- and submicron

81 SSA particles (Aller et al., 2017; Leck et al., 2013; Russell et al., 2010; Zeppenfeld et al., 2021a), most

82 likely resulting from their emission from the surface of the ocean after bubble bursting as part of jet

83 and film droplets (Veron, 2015; Wang et al., 2017). In addition to the bulk surface seawater, the sea

84 surface microlayer (SML) as the uppermost layer of the oceanic water column is an important source

85 of OM, and thus marine carbohydrates, in the SSA. The SML is described as a gelatinous film on top of

86 the ocean, which is often enriched in surface-active substances or buoyant gel particles compared to

87 the underlying bulk water (Engel et al., 2017; Wurl et al., 2009, 2011; Zäncker et al., 2017). Entrained

88 air bubbles rise within the upper part of the water column collecting surface-active organics on the

89 bubble surfaces from the bulk seawater (Burrows et al., 2014). Eventually they pass the thin SML and

90 burst there releasing film and jet droplets containing a mixture of substances found within the bulk

91 water and the SML (Burrows et al., 2014). At the same time, surfactants, exopolymers and microgels

92 in the SML increase the stability of the cap films of the bubbles, extend their lifetimes and enable the

93 drainage of water-soluble compounds (Bigg and Leck, 2008; Bikerman, 2013; Sellegri et al., 2006).

94 Consequently, the sea-air transfer occurs in a chemo-selective manner leading to a strong size-

95 dependent enrichment of surface-active organics relative to water-soluble sodium (Na^+) and, hence, a

96 relative chemical composition of SSA different to the surface seawater (Facchini et al., 2008; O'Dowd

97 et al., 2004; van Pinxteren et al., 2017; Prather et al., 2013; Quinn et al., 2015; Triesch et al., 2021a, b).

98 These chemo-selective enrichments of organic substances in the SSA relative to bulk water, especially

99 in the submicron size range, usually exceed the enrichments in the SML by orders of magnitude (van

100 Pinxteren et al., 2017; Schmitt-Kopplin et al., 2012). The underlying mechanisms for the chemo-

101 selective sea-air transfer of carbohydrates, including co-adsorption, are complex and subject of several

102 recent and ongoing laboratory tank and modelling studies (Burrows et al., 2016; Hasenecz et al., 2020;

103 Schill et al., 2018; Xu et al., 2023). After their emission, fresh SSA particles, including the contained

104 carbohydrates, undergo atmospheric aging due to a not yet well-understood interplay of several

105 atmospheric processes, such as atmospheric acidification, abiotic radical chemistry and biological and

106 enzymatic modifications (Angle et al., 2021; Hasenecz et al., 2020; Malfatti et al., 2019; Trueblood et

107 al., 2019; Zeppenfeld et al., 2021a), potentially also altering their microphysical properties.

108 Besides SSA, high concentrations of marine carbohydrates in fog and low-level clouds in the marine

109 environment are plausible due to the high hygroscopicity of SSA serving as good CCN (Xu et al., 2022)

transferring OM from the particle into the liquid phase, the high water-solubility of carbohydrates, and cloud-borne microorganisms potentially forming carbohydrates in-situ (Matulová et al., 2014). Only a few studies conducted at field sites exposed to marine air masses measured certain subgroups of carbohydrates, such as primary saccharides (Dominutti et al., 2022) or transparent exopolymer particles (TEP) (Orellana et al., 2011; van Pinxteren et al., 2022) so far in fog/clouds. However, the sources of marine carbohydrates in marine ambient fog/clouds, including dFCHO$_{fog}$ and CCHO$_{fog}$, and their relationship to the bulk seawater, SML and aerosol particles still lack elucidation.

During the summer months, the chemical compounds of natural SSA and marine fog can be studied in the Arctic Ocean due to the low influence of long-range transported anthropogenic pollution (Bozem et al., 2019; Schmale et al., 2021). However, the presence and seasonal evolution of Arctic sea ice divides this pristine region into a complex ensemble of several sea-ice-related sea surface compartments. These encompass the open leads - sea ice fractures with variable widths ranging from several to hundreds of meters - and polynyas, which are larger, more persistent areas of open water within the pack ice. Furthermore, there is the ice-free ocean, the marginal ice zone (MIZ) defined by a sea ice concentration threshold between 15 and 80% (Rolph et al., 2020), and melt ponds forming and developing during the melting season on top of the ice floes. These environments are characterized by different chemical, physical and biological characteristics potentially influencing the quantity and properties of the SSA emitted. Recent studies observed, for instance, that the number and efficiency of Arctic INP are strongly dominated by the type of sea-ice-related sea surface compartments that the air masses had passed before sampling (Creamean et al., 2022; Hartmann et al., 2021; Papakonstantinou-Presvelou et al., 2022; Porter et al., 2022). However, the individual conclusions still appear controversial and might be biased by seasonal and interannual variabilities. Consequently, more systematic studies in the Arctic, also with regard to the chemical properties of the aerosol particles, are required to achieve more conclusive results.

To increase the knowledge about marine carbohydrates as important constituents of SSA and potential CCN and INP, we present here the results of a comprehensive field study conducted onboard the German icebreaker RV *Polarstern* from May to July 2017. We performed concerted measurements of bulk seawater, SML, size-resolved aerosol particles and fog water at different locations dominated by different sea-ice-related sea surface compartments (ice-free, leads/polynyas, MIZ, melt ponds) in the Arctic Ocean. All marine and atmospheric compartments are discussed and compared on absolute CCHO concentrations, calculated CCHO/Na$^+$ ratios, the relative monosaccharide contribution to CCHO and the occurrence of dFCHO. The complex nature of these primary emission mechanisms and subsequent atmospheric aging of marine CCHO in the Arctic Ocean are discussed in relation to our findings. Our Arctic results are collated with those from the Southern Ocean at the Antarctic peninsula

144   during the austral summer, as presented in Zeppenfeld et al. (2021a) following a similar experimental

145   design. While both polar locations are remote marine regions with comparable meteorological

146   conditions during the sampling periods, the presence of Arctic sea ice adds another dimension of

147   complexity to data interpretation.

2. Experimental

2.1 Study area and field sampling

Field samples were gathered during the PS106 (PASCAL/SiPCA) campaign (Macke and Flores, 2018; Wendisch et al., 2018) conducted from May to July 2017 on board the German icebreaker RV *Polarstern* in the Fram Strait, Barents Sea and central Arctic Ocean, including a period operating from a drifting ice station (03–16 June 2017).

Marine SML and corresponding bulk water samples were collected from various locations as shown in Figure SI 1. These include the ice-free ocean (four sampling events), open water areas within the pack ice (20 sampling events, without distinguishing between open leads and polynyas), the MIZ (five sampling events), and young and aged melt ponds (six sampling events). Using visual characteristics, melt ponds were categorized as young (small, bluish, clear) or aged (larger, darker blue to greenish, and turbid with particulates and microalgae). To minimize contamination from exhausts and wastewater, water samples were taken at distances greater than 100 m from the ship. Seawater was collected either using a rubber boat or directly from the ice edge. SML samples were obtained by immersing a glass plate (length: 50 cm, width: 20 cm, thickness: 0.5 cm, sampling area: 2000 cm^2) vertically into the surface water and slowly withdrawing it at a speed of approximately 15 cm s^{-1} (van Pinxteren et al., 2012; Zeppenfeld et al., 2021a). The adhered SML film was drawn off the glass plate surface into a prewashed wide-neck plastic bottle by a framed Teflon wiper. The average thickness of the SML collected during this field study was 76±10 µm, which was calculated based on the volume of the SML sample collected, the area of the immersed glass plate and the number of dips as described by Cunliffe and Wurl (2014). Despite air temperatures during PS106 (median: -0.5°C; minimum: -7.6°C) hovering around or slightly below the freezing point of seawater, the SML remained unfrozen on the glass plate during sampling. The corresponding bulk water was taken from a defined depth of 1 m into LDPE bottles attached to a telescopic rod, except in the bottom closed melt ponds where it was scooped from the bottom at approximately 20–40 cm depth. Whenever melt pond sampling took place, snow samples were collected from the ice floe surface roughly 10 m away from the melt pond. Before each sampling, the sampling containers were first rinsed with a few milliliters of the corresponding aqueous sample which was disposed immediately after. On board, small aliquots of the water samples were analyzed immediately for salinity using a conductivity meter (pH/Cond 3320, WTW), colored dissolved organic matter (CDOM) and particulate absorption (PAB), with more details in section 2.6. For later chemical analyses (inorganic ions, pH, carbohydrates) 500–1000 mL of 0.2 µm filtered water sample (dissolved fraction), 0.2 µm polycarbonate filters (particulate fraction) and field blanks were stored at -20°C.

181   The sampling of ambient aerosol particles was conducted at the starboard side of RV *Polarstern* at the
182   top of the observation deck at a height of approx. 25 m above sea level as already described in Kecorius
183   et al. (2019). Size-segregated aerosol particles were sampled in five size ranges (stage 1: 0.05–0.14 µm,
184   stage 2: 0.14–0.42 µm, stage 3: 0.42–1.2 µm, stage 4: 1.2–3.5 µm, stage 5: 3.5–10 µm aerodynamic
185   particle diameter with a 50% cut-off) on aluminum foils by using two synchronized low-pressure Berner
186   impactors (Hauke, Austria) with a flow rate of 75 L min^{-1} and a sampling time of three to six days. To
187   avoid the condensation of atmospheric water and subsequent microbial activities on the aluminum
188   foils, a 3 m long heated tubes between the isokinetic inlets and the impactors reduced the relative
189   humidity of the sampled air to 75-80%, when the ambient relative humidity was higher. During this
190   field study, the difference of the temperatures of the ambient air at the inlet and the sampled air after
191   the heating never exceeded 9 K. Consequently, losses of semi-volatile compounds or changes by heat-
192   induced chemical reactions are expected to be neglectable. Furthermore, the Berner impactors were
193   thermally insulated by a polystyrene shell. After sampling, the foils were stored in aluminum containers
194   at -20°C until analysis. In this study, the results from stages 1-3, 4-5 and 1-5 were summed up as
195   submicron (sub), supermicron (super) and PM_{10}, respectively. Details about the size-resolved aerosol
196   particle samples and corresponding meteorological information are given in (**Table SI 1**, in total 15
197   complete sets of Berner foils).

198   Close to the aerosol sampling, fog was collected using the Caltech Active Strand Cloud Collector Version
199   2 (CASCC2) as described by Demoz et al. (1996). Bulk fog droplets were impacted on Teflon strands
200   with a diameter of 508 µm and collected into a prewashed Nalgene polyethylene bottle. The flow rate
201   was 5.3 m^3 min and the 50% lower cut-off was determined to be approximately 3.5 µm. Further
202   information about the 22 fog samples collected during the PS106 campaign including meteorological
203   information can be found in **Table SI 2** and in Hartmann et al. (2021).

2.2 Total aerosol particle mass concentrations

205   Before and after sampling, the aluminum foils were equilibrated (three days, 20°C, 50% relative
206   humidity) and weighed using a precise microbalance (Mettler Toledo XP2U, weighing error: ±4.6 µg).
207   Total particle mass concentrations (mass$_{aer, stage\ y}$) were calculated for each Berner stage as the ratio
208   between the difference of the absolute foil masses after and before sampling and the sampled air
209   volume. Afterwards, aluminum foils were divided for further chemical analyses.

2.3 OC/EC in aerosol samples

211   Organic carbon (OC$_{aer}$) and elemental carbon on Berner aerosol foils were determined as described by
212   Müller et al. (2010) using a two-step thermographic method (C/S MAX, Seifert Laborgeräte, Germany)
213   with a nondispersive infrared sensor.

2.4 Carbohydrates in aerosol particles, fog, snow, seawater and melt ponds

Marine carbohydrates in the particulate (pCCHO, >0.2 µm) and dissolved (dCCHO/dFCHO, <0.2 µm) phases, including truly dissolved molecules and small colloids, were quantified from seawater and melt pond samples following the protocol presented by Zeppenfeld et al. (2020, 2021a) using high-performance anion-exchange chromatography with pulsed amperometric detection (HPAEC-PAD) equipped with a Dionex CarboPac PA20 analytical column (3 mm × 150 mm) and a Dionex CarboPac PA20 guard column (3 mm × 30 mm). The monosaccharides fucose (Fuc), rhamnose (Rha), arabinose (Ara), galactose (Gal), glucose (Glc), xylose (Xyl), mannose (Man), fructose (Fru), galactosamine (GalN), glucosamine (GlcN), muramic acid (MurAc), galacturonic acid (GalAc), and glucuronic acid (GlcAc) were identified by their retention times. dFCHO represent the sum of identifiable monosaccharides before, and dCCHO and pCCHO additionally released after an acid hydrolysis (0.8 M HCl, 100°C, 20 h). CCHO is the sum of dCCHO and pCCHO. CHO represents the sum of CCHO and dFCHO, and consequently encompasses all carbohydrates measured within this study. **Figure 1** gives an overview of the here used carbohydrate-related abbreviations. Marine carbohydrates in fog water, snow and extracts from size-resolved aerosol particles were measured with (CCHO$_{fog}$, CCHO$_{aer}$) or without (dFCHO$_{fog}$, dFCHO$_{aer}$) prior acid hydrolysis.
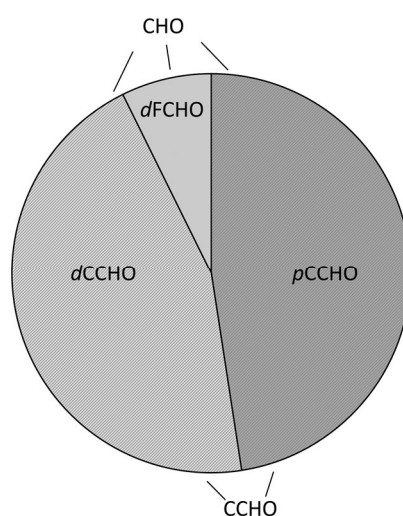
Figure 1. Overview of the abbreviations for carbohydrates (CHO) in seawater. CCHO: combined carbohydrates; pCCHO: particulate combined carbohydrates, dCCHO: dissolved combined carbohydrates; dFCHO: dissolved free carbohydrates.

2.5 Sodium and pH in aerosol particles, fog, seawater and melt ponds

Major inorganic ions, including sodium (Na$^+$), were determined from 0.45 µm filtered aqueous extracts of the size-resolved aerosol samples (50% of the Berner foil in 2 mL ultrapure water), fog water, diluted (1:15 000) seawater and melt pond samples using ion chromatography (ICS-3000, Dionex) as described by Müller et al. (2010). In this study, we discuss the results for Na$^+$ as a proxy for SSA emissions in remote marine regions. Additionally, the pH was monitored by an additional autosampler sample

243 conductivity and pH accessory (Dionex) in all seawater, melt pond and, whenever enough sample
244 volume was available, in fog water.

2.6 Absorption by phytoplankton, non-algal particles and colored dissolved organic matter in seawater and melt pond samples

247 For the investigation of bio-optical parameters in seawater and melt pond samples, the particulate
248 fraction was collected by filtering the water samples (5–500 mL) onto glass-fiber filters (GF/F,
249 Whatman), while the dissolved fraction was filtered through 0.2 µm Spartan syringe filters (Whatman,
250 Germany) immediately after sampling. The GF/F filters were analyzed to determine the absorption
251 spectra (i.e. 320–844 nm, 2 nm resolution) using the quantitative filtration technique with an
252 integrative-cavity absorption meter setup (QFT-ICAM) as developed by Röttgers et al. (2016). We
253 followed the protocol by Liu et al. (2018) for the instrument used here and the determination of the
254 absorption coefficients by total particles (a_p440), phytoplankton (a_{ph}440) and non-algal particles
255 (a_{NAP}440) at λ=440 nm.

256 The absorption for the dissolved fraction ($a_{CDOM}(λ)$) between 270 and 750 nm (1 nm resolution) were
257 measured as triplicates using a long path length liquid waveguide capillary cell (LWCC) system following
258 the procedure by Lefering et al. (2017) and including the correction for salinity effects by Röttgers et
259 al. (2014) as described for our instrumentation in Álvarez et al. (2022). The absorption coefficients in
260 the visible at 443 nm (a_{CDOM}443) and UV at 350 nm (a_{CDOM}350) bands were used as indicators of CDOM
261 magnitude.

2.7 Supporting observations

263 The German research vessel *Polarstern* performs continuous meteorological surface measurements
264 during times of ship operation. For this study, we used the data from the HMP155
265 thermometer/hygrometer probe (Vaisala), the ultrasonic anemometer (Thies Clima) and the FS11
266 visibility sensor (Vaisala) installed at a height of 29 m, 39 m and 20 m above sea level, respectively. The
267 quality-controlled data made available by the operators on the public repository PANGAEA
268 (Schmithüsen, 2018, 2019) supported the interpretation of the results of this study.

269 The 120 h back-trajectories were computed for the sampling periods of the size-resolved aerosol
270 particles and fog water events using the NOAA HYSPLIT model (Stein et al., 2015). The back-trajectories
271 were calculated on an hourly basis using the GDAS1 meteorological fields (Global Data Assimilation
272 System; 1° latitude/longitude; 3-hourly) and at arrival heights of 50, 250 and 1000 m. Sea ice
273 concentration data were retrieved from ERDDAP (Environmental Research Division's Data Access
274 Program), a data server maintained by NOAA (National Oceanic and Atmospheric Administration). The
275 MIZ was defined here as the oceanic region with a sea ice concentration between 15 and 80%. Data

on melt pond fractions were accessed from the sea ice remote sensing data achieve of the University of Bremen (https://data.seaice.uni-bremen.de, Istomina (2020)).

2.8 Statistics, calculations and visualization

Statistical analyses, calculations and visualization were performed in OriginPro, Microsoft Excel and R version 4.2.1 using the following packages: oce, ocedata, ncdf4, openair, ggplot2, reshape2, scales, lubridate, cmocean, maps, mapdata, rgdal, raster, RColorBrewer, sp. Time-resolved back-trajectories and sea ice maps were combined using R to compute and visualize the air mass history regarding the sea-ice-related sea surface compartments that have been passed. As a result, relative residence times of the air masses over certain surface features (ice-free, MIZ, pack ice, land) 12 hours before sampling were calculated based on defined thresholds for sea ice concentration: less than 15% for ice-free ocean, 15-80% for MIZ and over 80% for pack ice. Based on the remote sensing data used, we did not distinguish between open leads and melt ponds as the air traversed the pack ice. Box-whisker plots represent the interquartile range (box), median (horizontal line within the box), average (open square) and the minimum and maximum values of the datasets (whiskers). Measured mean values are given together with the calculated standard deviations (±). Correlations between two measured variables were expressed via the Pearson correlation coefficient R. The thresholds of significance were set for the p-values 0.1, 0.05, 0.01 and 0.001.

Enrichment factors for CCHO in the SML (EF_{SML}) relative to the corresponding bulk sample in different sea-ice-related sea surface compartments (ice-free, leads/polynyas, MIZ, melt ponds) were calculated based on **Formula 1** with $[x]_{SML}$ and $[x]_{bulk}$ representing the concentrations of either pCCHO or dCCHO. For the calculation of enrichment factors of CCHO in aerosol particles on Berner stage y ($EF_{aer,stage\ y}$; **Formula 2**) and fog water (EF_{fog}; **Formula 3**) relative to the bulk water samples, the ocean was assumed as the most likely source of atmospheric Na^+. For the calculations of EF_{aer} and EF_{fog}, we used the median value of all $CCHO_{bulk}$ /Na^+_{bulk} ratios found in the samples of a certain sea-ice-related sea surface compartment (ice-free, leads/polynyas, MIZ, melt ponds) over the whole campaign.

$$EF_{SML} = \frac{[x]_{SML}}{[x]_{bulk}} \tag{1}$$

$$EF_{aer,stage\ y} = \frac{[x]_{aer,stage\ y}/[Na^+]_{aer,stage\ y}}{[x]_{bulk}/[Na^+]_{bulk}} \tag{2}$$

$$EF_{fog} = \frac{[x]_{fog}/[Na^+]_{fog}}{[x]_{bulk}/[Na^+]_{bulk}} \tag{3}$$

3. Results and Discussion

The sources of SSA particles, and hence of atmospheric marine carbohydrates, microbial cells and fragments, in the Arctic are diverse and influenced by the prevailing sea ice conditions. Here, we present the concentrations and relative compositions of CCHO in the SML and bulk water from the ice-free ocean, open leads and polynyas within the pack ice, melt ponds and the MIZ. After this, the different sea-ice-related sea surface compartments are linked with the atmospheric CCHO found in ambient size-resolved aerosol particles and fog water. The influences of the air mass history, enrichments of CCHO towards Na^+ during the sea-air transfer and secondary atmospheric transformations processes altering atmospheric CCHO are discussed.

3.1 Sea ice influences the properties of the sea surface water

Variable CCHO concentrations in the Arctic surface water. CCHO were found in the dissolved (dCCHO) and particulate (pCCHO) phases of the SML and bulk water samples collected from the ocean and the melt ponds during the PS106 campaign. Among all aqueous samples, regardless of the sampling environment and depth (SML versus bulk), dCCHO (13–640 µg L^{-1}; mean$_{d\text{CCHO}}$ = 82±110 µg L^{-1}; n=70) and pCCHO (4–810 µg L^{-1}; mean$_{p\text{CCHO}}$ = 84±160 µg L^{-1}; n=70) concentrations were highly variable. However, the minimum, maximum and mean values of both dCCHO and pCCHO ranged within the same orders of magnitude. CCHO as the sum of dCCHO and pCCHO ranged between 22–1070 µg L^{-1} (mean$_{\text{CCHO}}$ = 166±250 µg L^{-1}; n=70).

Large differences in the mean values and standard deviations of CCHO were observed among the four sea-ice-related sea surface compartments in the Arctic (leads/polynyas within the pack ice, MIZ, ice-free ocean, melt ponds) as shown in **Figure 2a+b**. The highest mean values for dCCHO and pCCHO were observed in the SML of the MIZ (mean$_{d\text{CCHO, SML, MIZ}}$ = 190±160 µg L^{-1}; mean$_{p\text{CCHO, SML, MIZ}}$ = 370±310 µg L^{-1}; n=5) and melt ponds (mean$_{d\text{CCHO, SML, melt ponds}}$ = 190±240 µg L^{-1}; mean$_{p\text{CCHO, SML, melt ponds}}$ = 200±310 µg L^{-1}; n=6), while the SML of the lead/polynya (mean$_{d\text{CCHO, SML, lead/polynya}}$ = 70±75 µg L^{-1}; mean$_{p\text{CCHO, SML, lead/polynya}}$ = 70±120 µg L^{-1}; n=20) and ice-free open ocean (mean$_{d\text{CCHO, SML, ice-free}}$ = 73±12 µg L^{-1}; mean$_{p\text{CCHO, SML, ice-free}}$ = 36±5 µg L^{-1}; n=4) samples tended to contain less CCHO. The lower SML concentrations from this study for the Arctic ice-free open ocean and lead/polynya samples align closely with several other investigations. Specifically, our results are comparable to Gao et al. (2012), who studied the SML of Arctic leads (mean$_{d\text{CCHO, SML, Arctic leads}}$ = 163±104 µg L^{-1}; mean$_{p\text{CCHO, SML, Arctic leads}}$ = 35±25 µg L^{-1}; n=4), and Zeppenfeld et al. (2021), focusing on the ice-free part of the Southern Ocean west of the Antarctic peninsula during the austral summer (mean$_{d\text{CCHO, SML, Southern Ocean}}$ = 48±63 µg L^{-1}; mean$_{p\text{CCHO, SML, Southern Ocean}}$ = 72±53 µg L^{-1}; n=18). Similarly, our data mirror findings from the tropical Cape Verde (mean$_{d\text{CCHO, SML, Cape Verde}}$ = 85±30 µg L^{-1}; van Pinxteren

338   et al., 2023) and the Peruvian upwelling region (mean$_{d\text{CCHO, SML, Peru}}$ ≈ 92±32 µg L^{-1}; Zäncker et al., 2017).

339   Consequently, the Arctic MIZ and melt ponds, especially the aged ones with advanced microbiological

340   activities, stood out with elevated CCHO within the Arctic and also compared to tropical and other

341   polar regions.
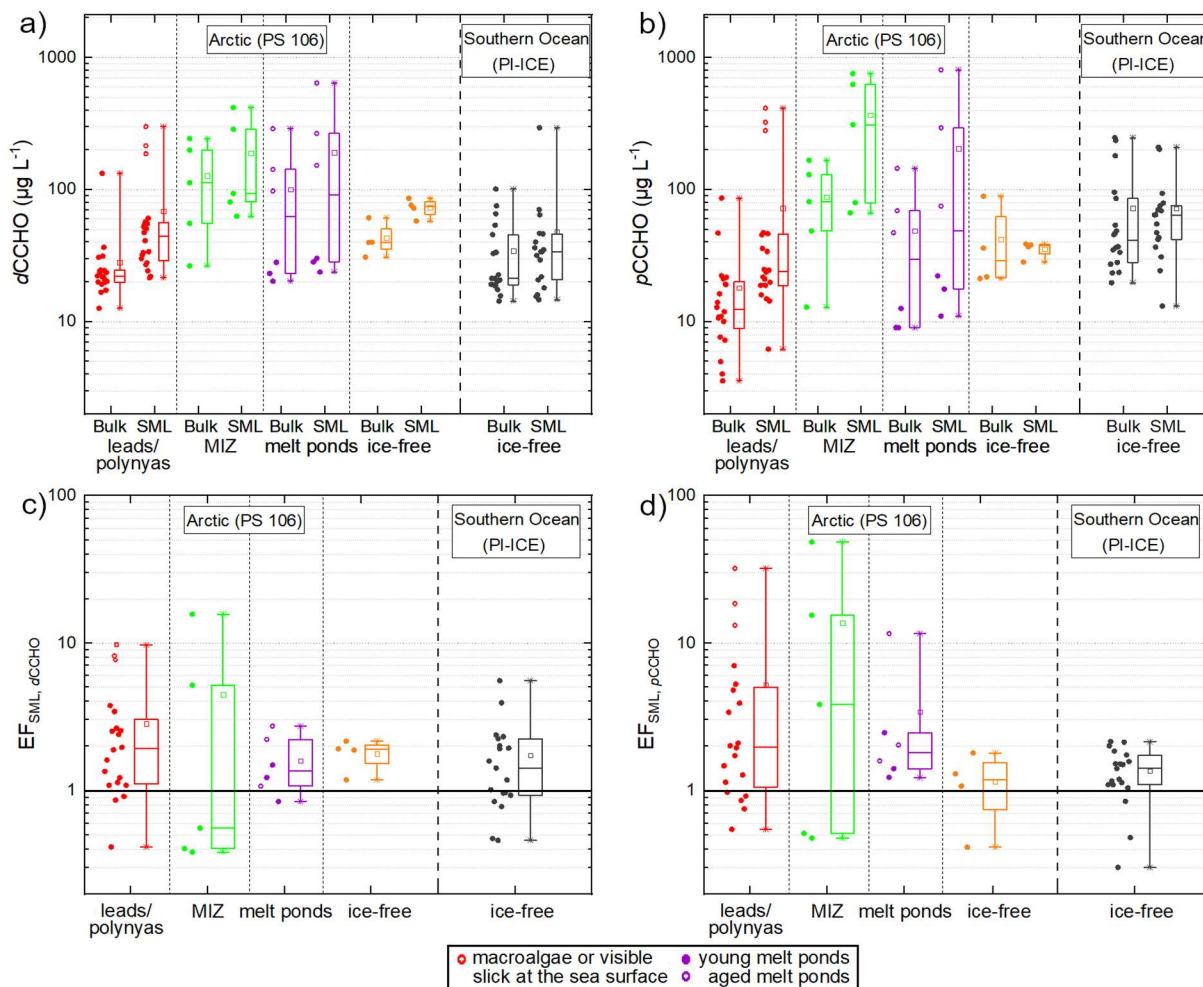
Figure 2. Scattered box-whisker plots showing the concentrations of a) dCCHO and b) pCCHO in the bulk and SML samples from the open leads and polynyas in the pack ice (red), the MIZ (green), ice-free open ocean (orange) and young and aged melt ponds (purple) collected during the PS106 campaign in the Arctic in comparison to the ice-free part of the Southern Ocean west of the Antarctic Peninsula investigated during the PI-ICE campaign in 2019 (black) as published in Zeppenfeld et al. (2021). EFs between SML and bulk water are shown in c) for dCCHO and d) for pCCHO. The black horizontal line represents an EF=1 meaning no enrichment or depletion.

342   ***Variable enrichments of CCHO in the SML.*** The enrichment factors (EF$_{SML}$) of the CCHO in the SML

343   relative to the corresponding bulk water ranged between 0.4 and 16 for dCCHO (**Figure 2c**), while the

344   EF$_{SML}$ for pCCHO varied between 0.4 and 49 (**Figure 2d**). 80% of the SML samples were moderately or

345   highly enriched in marine carbohydrates with only a few cases of depletion (7 for dCCHO and 8 for

346   pCCHO out of 35 in total). With a median EF$_{SML,pCCHO,MIZ}$ value of 3.8 and a mean of 13.8, the enrichment

347   of pCCHO in the MIZ stood out compared to the pCCHO in other sea-ice-related sea surface

348   compartments and to dCCHO overall. However, it should be noted that the number of MIZ samples

349   was low and median and mean values were dominated by three sample pairs with very high EF$_{SML}$

values. Low to moderate enrichments for dCCHO and pCCHO were typically found in the lead/polynya samples from the pack ice (median $EF_{SML,dCCHO,leads/polynyas}$=1.9; median $EF_{SML,pCCHO,leads/polynyas}$=2.0, n=20). However, three lead samples showed quite high dCCHO & pCCHO concentrations in the SML compared to the corresponding bulk samples resulting in high $EF_{SML,dCCHO,leads/polynyas}$ up to 10 and $EF_{SML,pCCHO,leads/polynyas}$ up to 32. The exceptionally high EFs of these three samples can be explained by the observation of slicks - visible films on the sea surface with altered reflectance and typically high enrichments of organics (Cunliffe et al., 2013; Stolle et al., 2010; Williams et al., 1986; Wurl et al., 2009) as well as the presence of macroalgae floating at the ocean's surface near the sampling site. Even though the macroalgae were not collected themselves, their exudates or fragments might have been released, accumulated and distributed in the SML close-by and thus sampled. Consequently, the few samples with high EFs in open leads might rather represent exceptional events as spatially small-scale phenomena.

The slight to high enrichments for dCCHO and pCCHO in this study are in good agreement with the values reported by Gao et al. (2012), who determined $EF_{SML,dCCHO}$ between 3.5 and 12, and $EF_{SML,pCCHO}$ between 1.7 and 7.0 for open leads within the central Arctic Ocean. Furthermore, the $EF_{SML,dCCHO}$ of the four Arctic sea-ice-related sea surface compartments reported here were not significantly different compared to values found in the ice-free part of the Southern Ocean (ANOVA, one-way, 0.05 significance level). For the pCCHO, however, the average EF_{SML} in the Arctic MIZ was significantly higher than the one of the Southern Ocean, whereas the $EF_{SML,pCCHO}$ of the ice-free ocean in the Arctic were similar to the Southern Ocean.

For explaining the accumulation in the SML, previous studies proposed several mechanisms and processes, which fundamentally differ for the dissolved and particulate carbohydrates. The enrichment of pCCHO in the SML might be dominated by an interplay of density-related and wind-driven processes. For instance, the positive buoyancy of TEP, a subgroup of pCCHO, leads to an upward flux serving as a continual vehicle for marine organisms and attached chemical compounds (Azetsu-Scott and Passow, 2004; Mari et al., 2017). Furthermore, strong winds can cause a short-term mixing of the upper water column reducing the EF_{SML} of particulates (Obernosterer et al., 2008) or TEP (Wurl et al., 2009; Zäncker et al., 2021), while the wind-induced entrainment of air and the bubbling of seawater convert dissolved negatively charged dCCHO and colloids into larger aggregates due to their sticky properties leading to an enrichment of pCCHO in the SML (Passow, 2002; Robinson et al., 2019; Wurl et al., 2011). The enrichment of dCCHO and also dFCHO in the SML is attributed to co-adsorption to other surface-active compounds from the seawater matrix being scavenged at the surface of rising bubbles (Burrows et al., 2016; Hasenecz et al., 2020; Schill et al., 2018; Xu et al., 2023). Additionally, microbial processes in the SML could enhance the enrichment through in-situ dCCHO production by micro- or macroalgae, while

384 photolysis and enzymatic degradation of dCCHO into dFCHO by heterotrophic bacteria could decrease

385 the SML enrichment. Specific to the Arctic, the release of meltwater from the sea ice could be an

386 additional source for carbohydrates in the SML, considering the production of CCHO, exopolymeric

387 substances (EPS) and TEP by sea ice algae and bacteria as a protection strategy against freezing damage

388 and fluctuating salinity in sea ice (Aslam et al., 2016; Krembs et al., 2002; Krembs and Deming, 2008).

389 This aligns well with the finding by Galgani et al. (2016) who observed labile, fresh OM in the SML of

390 melt ponds compared to the rather old, refractory nature of the SML in the surrounding open leads.

391 Hence, melting of sea ice could explain the extraordinarily high EF_{SML} observed in some, but not all,

392 SML samples from the MIZ and melt ponds. In summary, several processes might be responsible for

393 enrichment processes in the SML, especially in the Arctic, where the melting of sea ice could strongly

394 bias the physiochemical processes usually observed in controlled tank experiments.

395 ***High and low salinities due to freezing and melting of sea ice.*** While the surface seawater of the Arctic

396 Ocean is very saline, the Arctic sea ice is much fresher due the separation into salt-free ice crystals and

397 a salty brine during its formation from seawater and a subsequent salt loss from gravity drainage in

398 winter and flushing during summer (Notz and Worster, 2009). During the late spring and summer

399 period of this study, when strong melting of sea ice occurs, a large amount of freshwater enters the

400 surface of the ocean creating inhomogeneities of salinity within the surface of the ocean. In both the

401 ice-free ocean and the pack ice, where sea ice exists, but the melting rate is low, salinities of the SML

402 and the bulk water ranged in this study between 30.9 and 34.5 (Zeppenfeld et al., 2019b), which is

403 typical for the SML and the surface bulk water of the Arctic Ocean (Vaqué et al., 2021). Within the MIZ,

404 where freshwater from melting sea ice quickly mixes with the salty ocean water, salinities were similar

405 with values in this study between 30.1 and 33.4, however, also with an exception in the SML of 25.7.

406 Melt ponds that were not yet joined at the bottom with the ocean below, were much fresher with

407 lower and more variable salinities ranging from 4.3 to 19.5 (Zeppenfeld et al., 2019b). With a few

408 exceptions, salinity discrepancies between the SML and the corresponding bulk water were small in

409 most cases.

410 Sea-air transfer studies usually refer to open ocean scenarios with high salinities in the seawater and

411 without the presence of melting sea ice. For the calculation of enrichment factors of organics in aerosol

412 particles (EF_{aer}) or fog (EF_{fog}), the concentrations of Na^+ – a major compound of sea salt – in the

413 seawater bulk is included by default (see equations 2 and 3). However, the Arctic is a more complex

414 marine environment where salinities, and hence Na^+ concentrations, can vary widely as melting

415 progresses. This may strongly influence the mechanisms behind the bubble bursting process, the

416 $CCHO/Na^+$ ratios in the bulk seawater and the SML, and thus also the EF_{aer} and EF_{fog} as it will be

417   discussed in section 3.4. Consequently, the variability of salinity in Arctic seawater and melt ponds

418   should be considered for sea-air transfer studies that rely on Na^+ values.

419   ***Four sea-ice-related sea surface compartments with different characteristics.*** The high Arctic differs

420   from other oceanic regions in the presence, formation and melting of sea ice creating sea-ice-related

421   sea surface compartments (ice-free, leads/polynyas, MIZ, melt ponds) with individual biological and

422   chemical characteristics, such as CCHO concentrations, enrichments in the SML and salinities. This

423   might potentially impact the transfer of substances from the ocean to the atmosphere, chemo-

424   selective enrichment processes of marine CCHO in the primary marine aerosol particles and thus their

425   microphysical properties. The next sections will elucidate if and how these differences within the

426   individual compartments relate to $CCHO_{aer}$ and $CCHO_{fog}$.

3.2 Sea spray aerosol and therein contained combined carbohydrates

Breaking waves as the main mechanism for SSA emissions is not unambiguous in the Arctic. In the open ocean, the emission flux of SSA and hence its inorganic and organic constituents mainly depend on the wind speed as the driving force for breaking waves and bubble bursting, and furthermore on the seawater temperature, salinity, wave properties and organic surface-active substances (Grythe et al., 2014). In this study, atmospheric sodium ($Na^+_{aer,PM10}$), the best tracer for SSA (Barthel et al., 2019), ranged between 12 and 765 ng m^{-3} (**Table SI 1**). $Na^+_{aer,PM10}$ showed a good correlation (R=0.80, p<0.001, **Figure 3a**) with wind speed, measured at the sampling site and averaged over the sampling time, if all aerosol samples are included. However, the strength of this correlation decreased sharply (R=0.59, p<0.1), when only samples collected over the MIZ and the pack ice were included, while the few samples from the open ocean characterized by high Na^+ values were excluded. This is due to the presence of sea ice in the high Arctic, which likely alters and conceals the classical wind-driven mechanisms of breaking waves and bubble bursting resulting in SSA emission. Firstly, sea ice covers a significant part of the Arctic Ocean strongly reducing the area releasing SSA. Secondly, the presence of sea ice causes an attenuation of the high-frequency wind-sea waves, while longer waves, such as swells, can remain (Thomson, 2022). Consequently, the effect of wind on the SSA emission mechanisms within the open leads and the MIZ might be different than in the ice-free ocean. For those sea-ice-dominated compartments, alternative wind-independent sources of ascending bubbles were suggested, such as melting sea ice nearby, respiration of phytoplankton or sea-air heat exchange below the sea surface (Chen et al., 2022 and references therein). Thirdly, in contrast to other marine regions with quite homogeneous ocean salinities, and hence sodium concentrations, the salinities among the different Arctic sea-ice-related sea surface compartments are more variable due to the melting of sea ice. Previously, the results of a sea-air transfer tank experiment with artificial seawater showed the influence of salinity on the relative particle number concentrations of emitted SSA for salinities below 15 – values especially relevant for melt ponds in the Arctic – while changes at higher salinities did not result in a measurable effect (Zábori et al., 2012). Additionally, organics with potential surface-active properties are very variable in these disparate Arctic environments, as discussed for CCHO in section 3.1. Organic surfactants can alter the ocean surface's ability to form whitecaps and the lifetime of bubbles (Bigg and Leck, 2008; Callaghan et al., 2012; Grythe et al., 2014) and therefore SSA properties.

Finally, blowing snow over the sea ice could serve as an additional source of atmospheric Na^+_{aer} when a certain air-temperature-dependent wind speed threshold is exceeded. (Chen et al., 2022; Gong et al., 2023; Huang and Jaeglé, 2017; Yang et al., 2008). Consequently, connections and correlations for the release of SSA particles in the heterogeneous high Arctic are more difficult to explore than other

460   marine environments without sea ice. It can be assumed that this complex setting influences not only

461   the release of inorganic constituents from seawater, but also its organic compounds, such as CCHO.

462
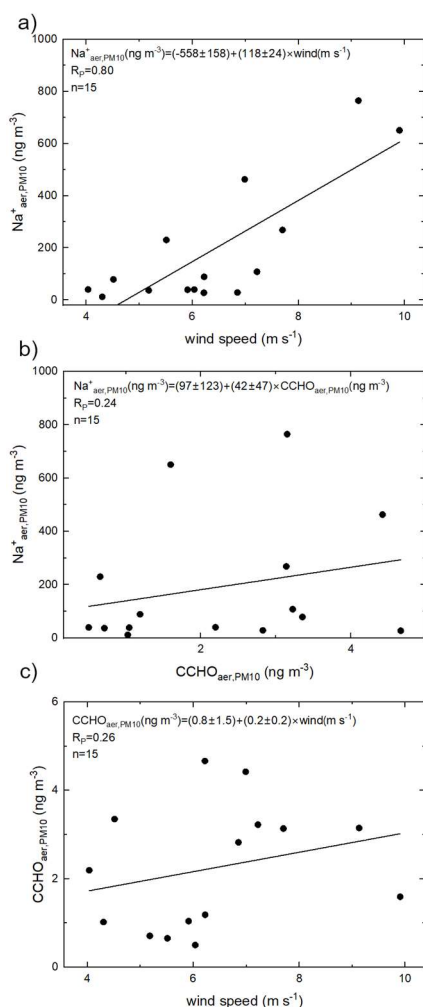
476   **Figure 3.** Correlations between a) $Na^+_{aer,PM10}$ and the averaged wind speed, b) $Na^+_{aer,PM10}$ and $CCHO_{aer,PM10}$, c) $CCHO_{aer,PM10}$ and averaged wind speed.

477   ***CCHO$_{aer}$ distributed in all size modes.*** During the PS106 campaign, the overall atmospheric

478   concentrations of $CCHO_{aer,PM10}$ ranged between 0.5 and 4.7 ng m^{-3} (**Table SI 1**). Combined

479   carbohydrates were found on both supermicron ($CCHO_{aer,super}$=0.07–2.1 ng m^{-3}) and submicron

480   particles ($CCHO_{aer,sub}$=0.26–4.4 ng m^{-3}). Thus, these $CCHO_{aer}$ values ranged within the same orders of

481   magnitude as in the Arctic studies by Karl et al. (2019) and Leck et al. (2013) or the study conducted at

482   the western Antarctic peninsula by Zeppenfeld et al. (2021a). $CCHO_{aer}$ appeared in all of the five size

483   classes in variable concentrations (**Figure 4a**). Although the average concentrations were similar on all

484   stages, local maxima were observed on stages 2 (0.14–0.42 µm) and 5 (1.2–10 µm). A similar size

485   distribution of marine $CCHO_{aer}$ in these specific size ranges, but more pronounced, has been already

486   observed in the ice-free part of the Southern Ocean by Zeppenfeld et al. (2021a) explaining these

487   findings with a likely release of marine polysaccharides from the ocean as part of film and jet droplets.

488   Possibly, the aerosol size distribution of marine polysaccharides resulting from wind-driven bubble

489   bursting emissions are not as obvious in this Arctic study as it was in the ice-free Southern Ocean due

490   to the presence of Arctic sea ice suppressing and altering the local SSA emission mechanisms as

491   indicated in the previous section. The relative contribution of $CCHO_{aer}$ to $mass_{aer}$ varied between 0.01%

492   and 4% (**Figure 4b**), while the carbon contained within the combined carbohydrates (C-$CCHO_{aer}$)

493   contributed 0.06 to 4.9% to the OC_{aer} in the size-resolved aerosol particles (**Figure 4c**). These

494   contributions agree well with the findings in marine aerosol particles from the Southern Ocean

495   (Zeppenfeld et al., 2021a).

496
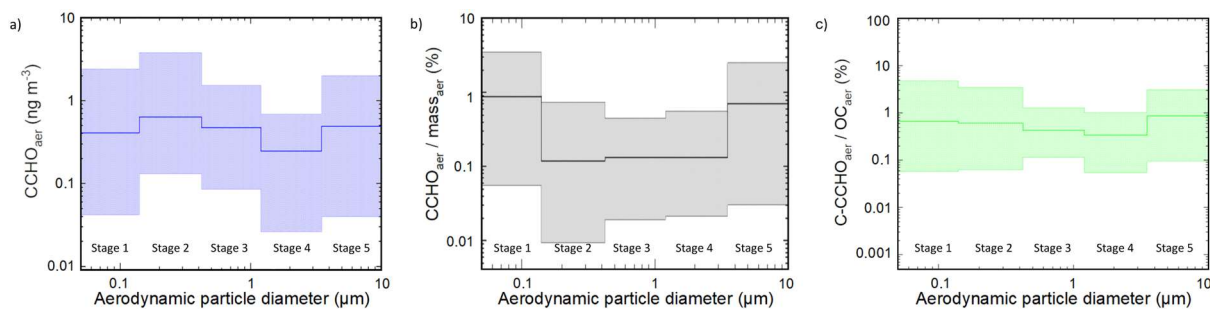
Figure 4. a) Concentration of combined carbohydrates in size-resolved aerosol particles ($CCHO_{aer}$), b) ratio of $CCHO_{aer}$ to the total particle mass concentration ($mass_{aer}$), c) ratios of carbon contained within the combined carbohydrates in aerosol particles (C-$CCHO_{aer}$) to organic carbon in aerosol particles (OC_{aer}). The bold lines represent the average concentrations during the PS106 campaign. The hatched areas show the range between the maximum and minimum values. The aerodynamic particle diameter refers to sampling conditions at relative humidity of max. 80%.

497   Unlike the study conducted in the Southern Ocean (Zeppenfeld et al., 2021a), $CCHO_{aer,PM10}$ in this study

498   showed no significant correlations with $Na^+_{aer,PM10}$ (R=0.24, p>0.1, **Figure 3b**) or wind speed (R=0.26,

499   p>0.1, **Figure 3c**). The presence of sea ice resulting in melt ponds and MIZ regions, and the interplay of

500   multiple emission mechanisms in the Arctic, as discussed earlier, could account for this complexity.

501   However, if the correlations are resolved for the different Berner impactor stages (i.e. size ranges), a

502   large variability can be observed (**Figure 5**). A higher correlation was found especially on stage 4

503   (1.2–3.5 µm) between $CCHO_{aer,stage\ 4}$ and $Na^+_{aer,stage\ 4}$ (R=0.76, p<0.01), while the Pearson correlations

504   coefficients for the other Berner stages were much lower. This could indicate the same marine source

505   and wind-driven emission mechanism for both chemical constituents in this supermicron aerosol size

506   mode, while other aerosol size modes might have been influenced by atmospheric aging and wind-

507   independent emission mechanisms as already mentioned for Na^+_{aer} in the previous section. This

508   observation agrees well with the findings by Bigg and Leck (2008) and Leck (2002) reporting submicron

509   polymer gel particles, likely consisting of polysaccharides, in the atmosphere of the high Arctic

510   containing almost no sea salt and showing large similarities to those particles found in open leads

511   close-by. This is quite surprising considering that the mechanism of wind-driven wave breaking is quite

512   limited due to the lack of long fetches of open water (Held et al., 2011; Norris et al., 2011).

513

514

515

516

517

518

519

520
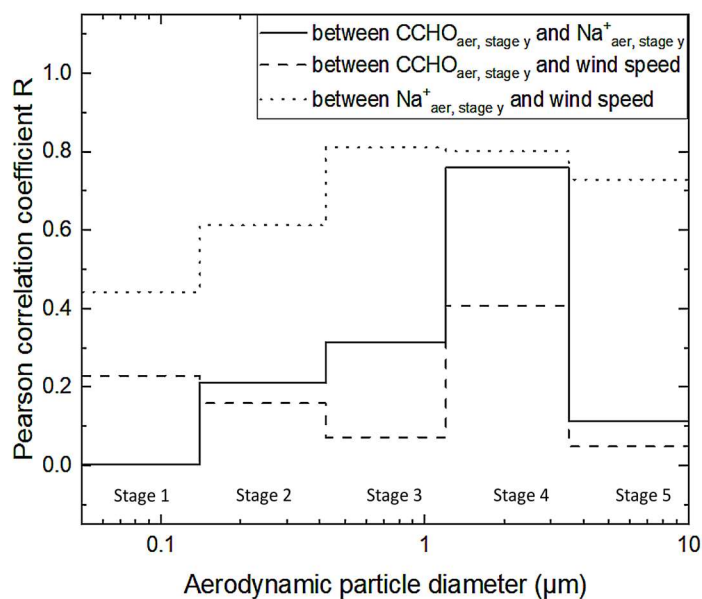
Figure 5. Pearson correlation coefficient R between CCHO$_{aer,stage\ y}$ and Na$^+_{aer,stage\ y}$ (solid line), between CCHO$_{aer,stage\ y}$ and the average wind speed (dashed line), and between Na$^+_{aer,stage\ y}$ and the average wind speed (dotted line) for each stage y of the Berner impactor.

521 Blowing snow has been discussed as a possible additional source for atmospheric Na$^+$, raising the

522 question, if it could be a source for atmospheric carbohydrates, too. During this study, the

523 measurements of dFCHO and CCHO in five Arctic snow samples collected resulting in low values mostly

524 below the limits of detection. This finding supports the conclusion that blowing snow does not serve

525 as a competitive source for the emission of atmospheric marine carbohydrates.

3.3 Marine combined carbohydrates in fog

The concentrations of $Na^+_{fog, liquid}$ (1.7–903 mg L^{-1}; mean = 130±220 mg L^{-1}; n=22) and $CCHO_{fog, liquid}$ (18–22000 µg L^{-1}; mean = 1380±4600 µg L^{-1}; n=22) were very variable in fog water (**Table SI 2**). Atmospheric concentrations of these chemical constituents in fog droplets (indicated by the index 'fog,atmos') can be calculated under consideration of the liquid water content (LWC) during the fog events. Since LWC was not measured during PS106 directly, the LWC was approximated from the measured CCN concentrations at the lowest quality assured supersaturation of 0.15% and an assumed average droplet diameter of 17 µm. This approach resulted in LWCs of 0.62 ±0.39 g m^{-3} for the fog collected over the North Sea and Norwegian Sea, and 0.10±0.09 g m^{-3} for the fog over the Arctic Ocean (Hartmann et al., 2021). Following this approach, atmospheric concentrations in fog ranged between 0.12 and 150 µg m^{-3} (mean = 25±43 µg m^{-3}; n=16) for $Na^+_{fog, atmos}$, and between 3 and 4300 ng m^{-3} (mean = 390±1100 ng m^{-3}; n=16) for $CCHO_{fog, atmos}$, respectively. These atmospheric concentrations in fog are for both $Na^+_{fog, atmos}$ and $CCHO_{fog, atmos}$ by one to three orders of magnitude higher than the atmospheric concentrations in aerosols discussed in section 3.2. This divergence may be explained by the following:

- Fog scavenging is a transfer process of aerosol particles into the liquid phase of fog droplets (Gilardoni et al., 2014). As fog forms and grows, it can capture aerosol particles in the air and increase their concentration within the fog droplets. This could lead to higher atmospheric concentrations of aerosol particle compounds, especially for the water-soluble and hygroscopic ones, inside the fog compared to the surrounding air.
- The activation of aerosol particles to fog droplets is a process dominated by particle size with larger particles tending to activate first. It is conceivable that SSA particles larger than 10 µm, usually few in number, but with a large mass contribution, were available near the sea surface, where sampling occurred. These SSA particles were activated into fog droplets and contributed significantly to the Na^+ and CCHO in the fog. In contrast, aerosol sampling was restricted by the Berner impactor's 10 µm diameter cut-off neglecting the larger particles in the consideration.
- The LWC values were not measured but estimated, which could be a source of errors. This approach resulted in values representing rather the upper limit of LWC values typically reported for Arctic summer fog (0.001-0.17 g m^{-3} (Kumai, 1973)) or sea fog (0.02-0.1 g m^{-3} (Herrmann et al., 2015)), but appear within a realistic range. Consequently, they are likely not responsible for the large difference between aerosol and fog concentrations of several orders of magnitude.

559 Since both, organic and inorganic constituents, showed higher atmospheric concentrations in
560 fog/clouds compared to ambient aerosol particles, we conclude that a physical phenomenon, such as
561 fog scavenging, might explain this observation and not an in-situ formation within the cloud droplets.
562 Similar to the findings of this study discussing marine CCHO and Na^+ in Arctic fog, Triesch et al. (2021a)
563 found strikingly high concentrations of free amino acids (FAA) and Na^+ in marine clouds compared to
564 aerosol particles both collected on top of the Mt. Verde on Cape Verde as shown in **Table 1**.

565 While dFCHO$_{fog}$ and derivatives, such as anhydrosugars and sugar alcohols, have been readily reported
566 for fog water with terrestrial and marine background (Dominutti et al., 2022), we here present for the
567 first time ambient CCHO concentrations in marine fog.

568 **Table 1.** Atmospheric concentrations of selected SSA constituents in fog/clouds compared to ambient aerosol particles during
569 marine field studies.

Chemical constituent	Fog/cloud	PM$_{10}$	Sampling location	Sampling height	Sampling period	Reference
	(ng m^{-3})	(ng m^{-3})		(m a.s.l.)[h]		
dFCHO	9.2—52[a,b]	—	Reúnion	1760[d]	March—April 2019	Dominutti et al. (2022)
	1.5—1040 (mean:80±260)	<LOD—2.0	Arctic	25[e]	May—July 2017	this study
CCHO	3—4300 (mean:390±1100)	0.5—4.7	Arctic	25[e]	May—July 2017	this study
FAA	11—490	1.0—4.8	Cape Verde	744[f]	Sept.—Oct. 2017	Triesch et al. (2021a)
	6—79[b]	—	Reúnion	1760[d]	March-April 2019	Dominutti et al. (2022)
	(µg m^{-3})	(µg m^{-3})		(m a.s.l.)[h]		
Na$^+$	1.6—7.2	0.17—0.40	Cape Verde	744[f]	Sept.—Oct. 2017	Triesch et al. (2021a)
	0.1—2.2[b]	—	Reúnion	1760[d]	March—April 2019	Dominutti et al. (2022)
	0.014—0.063[c]	—	Arctic	180-374[g]	Aug.—Sept. 2018	Zinke et al. (2021)
	0.12—150 (mean:25±43)	0.012—0.77	Arctic	25 m[e]	May—July 2017	this study

570 [a]only includes free glucose and rhamnose; sugar alcohols and anhydrosugars were not included for this table. [b]values were
571 calculated from LWCs, molecular weights and concentrations in fog water given within the reference; terrestrial contributions
572 are likely. [c]calculated from concentration in fog water and an assumed LWC of 0.1 g m^{-3}. [d]Piste Omega. [e]RV *Polarstern*. [f]Mt.
573 Verde. [g]tethered balloon, [h]'m a.s.l' abbreviates 'meters above sea level'.

3.4 Chemo-selective sea-air transfer of marine carbohydrates

The chemo-selective sea-air transfer of organics towards inorganic sea salt constituents has been described both in tank and ambient field studies for organic carbon in general (Gantt et al., 2011; Hoffman and Duce, 1976; van Pinxteren et al., 2017) or several chemical constituents, such as carbohydrates (Hasenecz et al., 2020; Schill et al., 2018; Zeppenfeld et al., 2021a), lipids (Triesch et al., 2021b) and free and combined amino acids (Triesch et al., 2021a, c).The calculation of dimensionless ratios between the concentrations of the examined organic parameter and Na^+ allows a comparison of aquatic and atmospheric samples within the marine environment. **Figure 6** shows the CCHO/Na^+ ratios for the bulk and SML in the four sea-ice-related sea surface compartments, size resolved aerosol particles and fog water collected during the PS106 cruise.
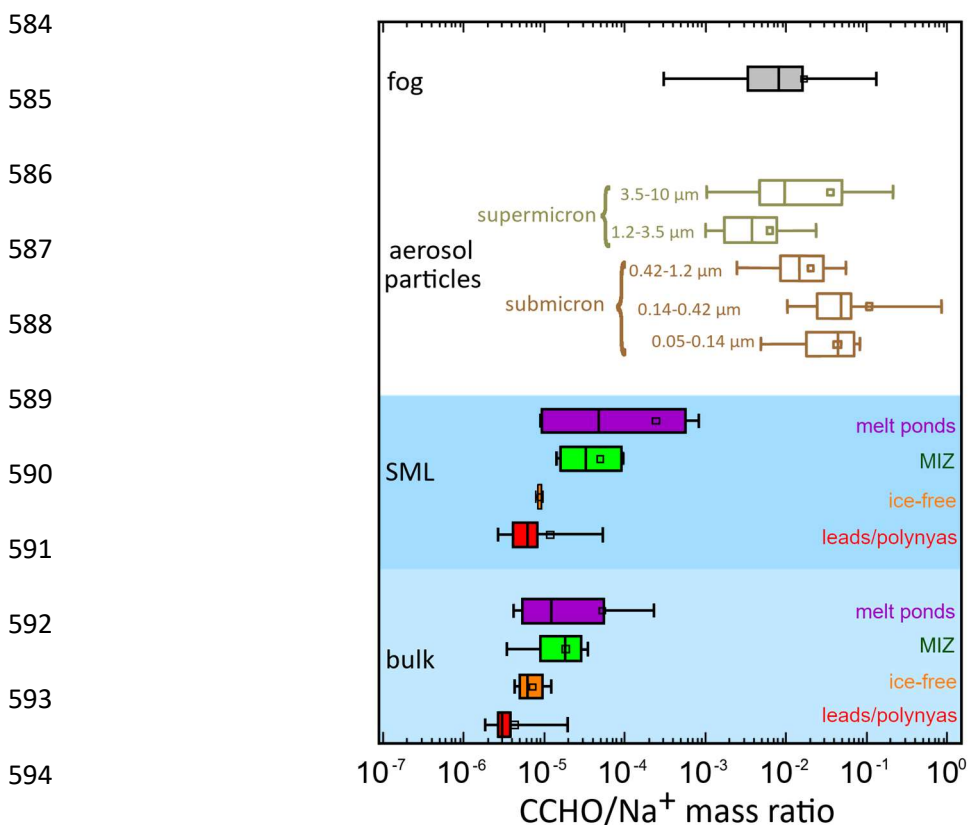
Figure 6. CCHO/Na^+ ratios for CCHO in Arctic fog, size-resolved aerosol particles and the surface seawater (SML and bulk) from melt ponds, the marginal ice zone (MIZ), the ice-free ocean and leads/polynyas from the pack ice.

Wide range of CCHO/Na^+ ratios in Arctic surface seawater. In the surface seawater samples of this study, the CCHO/Na^+ ratios spanned from 2×10^{-6} to 8×10^{-4}, representing a wider range than those found in the Southern Ocean (9×10^{-7} and 3×10^{-5}; Zeppenfeld et al., 2021). While the ratios in the SML and bulk water in general ranged in the same orders of magnitude, large differences were observed in the individual Arctic sea-ice-related sea surface compartments. In the SML, lowest median values were found in the leads/polynyas and ice-free ocean samples with 6×10^{-6} and 9×10^{-6}, respectively, while higher median values appeared in the SML of the MIZ (3×10^{-5}) and melt ponds (4×10^{-5}), or even

602   6×10^{-4}, when only aged melt ponds were considered. This large variability of CCHO/Na$^+$ ratios can be

603   explained by the variable content of CCHO (high CCHO content in aged melt ponds & MIZ versus lower

604   CCHO content in ice-free ocean & leads/polynyas) and Na$^+$ (low salinity in the SML of melt ponds versus

605   higher salinities in ice-free ocean & leads/polynyas & MIZ) in the different sea-ice-related sea surface

606   compartments. It can be expected, that the different CCHO/Na$^+$ ratios in the individual seawater

607   compartments impacted the corresponding CCHO/Na$^+$ ratios in fog and aerosol particles during the

608   sea-air transfer, and consequently the enrichment factors for the sea-air transfer (EF$_{aer}$, EF$_{fog}$), which

609   are calculated from those ratios.

610   ***Air mass history influences CCHO$_{aer}$/Na$^+_{aer}$ ratios in Arctic aerosol particles.*** In contrast to the

611   seawater samples, CCHO$_{aer}$/Na$^+_{aer}$ ratios were much higher for aerosol particles considering the size

612   resolution (1×10^{-3}–9×10^{-1}) supporting the concept of the chemo-selective enrichment of

613   carbohydrates towards Na$^+$ during the transfer from the ocean into the atmosphere. In this context,

614   submicron particles showed much higher median ratios of 4×10^{-2} (0.05–0.14 µm) and 4×10^{-2}

615   (0.14–0.42 µm) than supermicron particles with 4×10^{-3} (1.2–3.5 µm) and 1×10^{-2} (3.5–10 µm).

616   Regarding PM$_{10}$ (sum of all five Berner stages), the CCHO$_{aer,PM10}$/Na$^+_{aer,PM10}$ ratios varied much more in

617   the Arctic study presented here (2×10^{-3}–2×10^{-1}, see **Table SI 1**) than in the ice-free part of the Southern

618   Ocean (8×10^{-4}–7×10^{-3}; Zeppenfeld et al. (2021b)).

619   During four aerosol sampling periods (24/05/17–26/05/17; 26/05/17–29/05/17; 29/05/17–01/06/17;

620   19/06/17–25/06/17), air masses had predominantly passed over the ice-free ocean (45–100% of the

621   12 hours prior to sampling, as shown in **Table SI 1** & **Figure SI 2**). Interestingly, these periods exhibited

622   the lowest CCHO$_{aer,PM10}$/Na$^+_{aer,PM10}$ ratios (2×10^{-3}–9×10^{-3}, detailed in **Table SI 1**), values that are

623   strikingly similar to those observed in the ice-free Southern Ocean. In contrast, higher ratios were

624   found, when the air masses had rested a significant time over the pack ice or the MIZ. This could be an

625   indication that the chemical composition of the sea-ice-related sea surface compartments, here the

626   ice-free ocean with low CCHO/Na$^+$ ratios, strongly influences the relative composition of aerosol

627   particles. In contrast, the influence of the MIZ, pack ice and melt ponds exhibiting quite different

628   chemical, physical and biological properties on CCHO$_{aer,PM10}$/Na$^+_{aer,PM10}$ could not be resolved in further

629   details following this approach using back-trajectory calculations and satellite data. This is certainly

630   due to the proximity of these sea-ice-related sea surface compartments on a small spatial scale

631   (especially melt ponds in direct vicinity to open leads), the long sampling periods of aerosol particles,

632   the lacking knowledge of deposition rates, the effect of wind on wave propagation and bubble bursting

633   processes within the individual sea-ice-related sea surface compartments and missing data on the

634   biological activities in individual melt ponds.

Similar CCHO/Na+ ratios in aerosol particles and fog. For fog, $CCHO_{fog}/Na^+_{fog}$ ratios ranged from 3×10^{-4} to 1×10^{-1}, which covers the same orders of magnitude of aerosol particles. Even though absolute atmospheric concentrations of CCHO are much higher in fog than in aerosol particles possibly due to fog scavenging (as discussed in 3.3), the CCHO/Na+ ratios were similar. This strongly implies that $CCHO_{fog}$ actually originated from the ambient marine aerosol particles. The attempt to find matches or common trends between aerosol particles and the fog in individual samples was not successful, certainly due to the very different resolutions of sampling times and in addition due to the probability of fog droplets containing aerosol particles bigger than 10 μm.

Calculated EF_{aer} and EF_{fog} depend on the sea-ice-related marine source under consideration. EF_{aer} and EF_{fog} are calculated as a quotient between the CCHO/Na+ ratios in the size-resolved aerosol particles/fog and the corresponding bulk water. The CCHO/Na+ ratios in the Arctic seawater of this study were very variable depending on the regarded sea-ice-related sea surface compartment environment, as well in the aerosol particles and in fog water. This fact strongly impacted the resulting hypothetical EF_{aer} and EF_{fog}, enabling calculated values ranging between 10^1 and 10^4 for supermicron aerosol particles, between 10^2 and 10^5 for submicron particles and between 10^0 and 10^4 for fog depending on which sea-ice-related sea surface compartment was assumed as the marine source of SSA as shown in **Figure 7**. Due to missing information, including SSA emission fluxes from the four sea-ice-related compartments, aerosol deposition rates, biological activities in melt ponds, wind effects on wave propagation and bubble bursting, and the comparative importance of melt ponds versus open leads (which are in close proximity, making it difficult to resolve them in back-trajectory analyses) as SSA sources – we didn't perform calculations based on the back-trajectory history of each atmospheric sample. Instead, subsequent calculations for EF_{aer} and EF_{fog} employed a hypothetical approach, assessing the range of enrichment factors by considering only one of the four sea-ice-related compartments—represented by the corresponding median $CCHO_{bulk}/Na^+_{bulk}$ ratios—as the only source, while excluding the others.

Lower atmospheric EFs were calculated when aged melt ponds ($EF_{aer,super}$=19–750; $EF_{aer,sub}$=127–5100; EF_{fog}=5–2400) or the MIZ ($EF_{aer,super}$=60–2310; $EF_{aer,sub}$=390–16000; EF_{fog}=17–7400) were assumed as the only (theoretical) source of CCHO and Na+, while higher values were found with the ice-free ocean ($EF_{aer,super}$=175–6800; $EF_{aer,sub}$=1100–46000; EF_{fog}=50–22000) or open leads/polynyas ($EF_{aer,super}$=360–14000; $EF_{aer,sub}$=2360–95000; EF_{fog}=103–44600). It is important to note that EFs were most consistent with results from other CCHO sea-air transfer studies in the tank (Hasenecz et al., 2020) and the field (Zeppenfeld et al., 2021a), when aged melt ponds or the MIZ were considered as the only emission source. If leads/polynyas and the ice-free ocean were regarded as the only emission source, higher EF_{aer} and EF_{fog} values were obtained, and hence a possible overestimation of the

669 mechanistic process of enrichment. As the results on back-trajectory calculations and sea ice maps

670 demonstrated (Table SI 1 & Figure SI 2), most air masses were exposed to several of the sea-ice-related

671 sea surface compartments before sampling. Consequently, none of the Arctic sea-ice-related sea

672 surface compartments discussed above should be overlooked when discussing of sea-air transfer of

673 organic substances.

674 During the same Arctic field campaign, Hartmann et al. (2021) investigated INP in ambient aerosol

675 particles and compared it to bulk and SML in seawater from all the different sea-ice-related sea surface

676 compartments using similar EF_{aer} calculations as reported here. They concluded that an enrichment of

677 3 to 5 orders of magnitude was necessary during the sea-air transfer to fully attribute atmospheric INP

678 to oceanic sources. Here, we show that such high EF_{aer} and EF_{fog} for organics, and hence marine

679 biogenic INP, can be calculated, e.g. when open leads/polynyas were referred to as the only oceanic

680 source. In summary, Artic air masses have been impacted by different types of sea-ice-related sea

681 surface compartments before sampling, whereas it is still unclear which one has the biggest effect on

682 the chemical composition of the marine aerosol particles. This aspect should be considered when the

683 marine SSA constituents are modelled for the Arctic from remote sensing data.

684
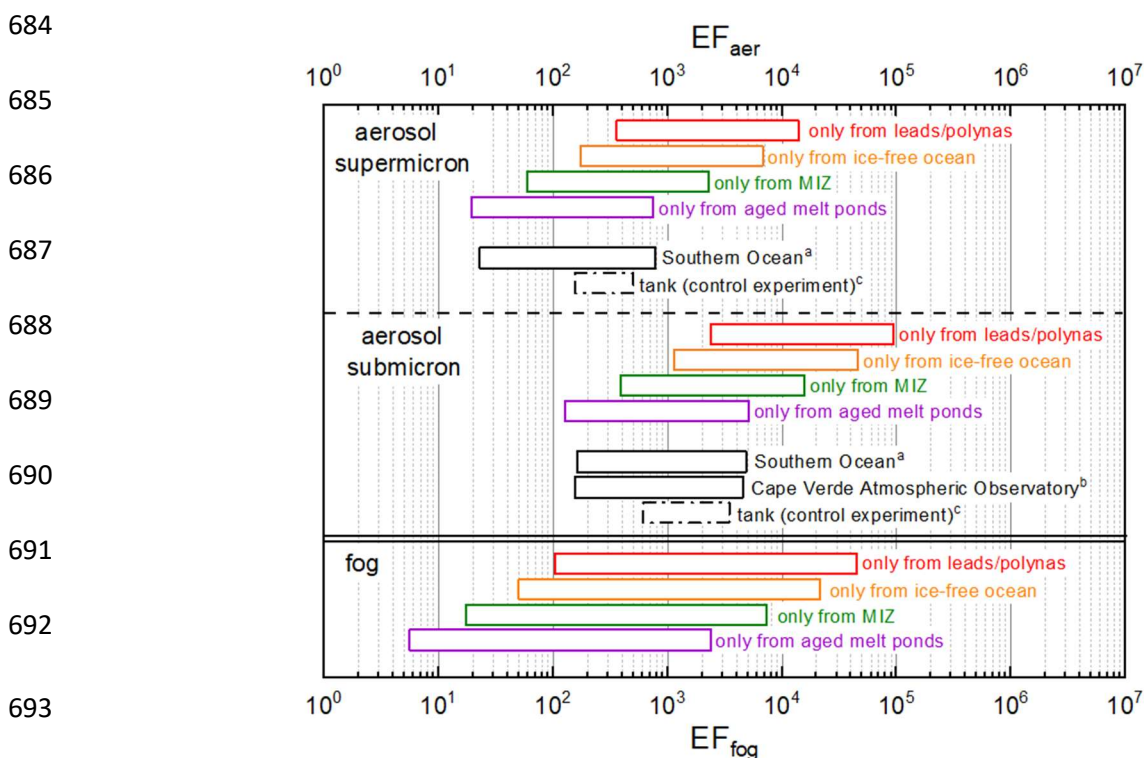
Figure 7. Range of calculated hypothetical enrichment factors EF_{aer} and EF_{fog} assuming either leads/polynyas, the ice-free ocean, the MIZ or aged melt ponds as the only marine source for the sea-air transfer of CCHO in the Arctic. For the calculation of EF_{aer} and EF_{fog}, the minimum and maximum values of the $CCHO_{aer/fog}/Na^+_{aer/fog}$ ratios and the median values of $CCHO_{bulk}/Na^+_{bulk}$ were used. The EF_{aer} values of this study were compared with the results of a) the field study conducted in the Southern Ocean by Zeppenfeld et al. (2021), b) the field study conducted at Cape Verde Atmospheric Observatory (CVAO) by van Pinxteren et al. (2023) and c) the results of the CCHO tank study by Hasenecz et al. (2020) without any addition of heterotrophic bacteria (control experiment). Here, EF_{aer} values were calculated from the experimental data published by Hasenecz et al. (2020b).

3.5 Atmospheric aging of marine carbohydrates

To resolve the fate of marine carbohydrates in the atmosphere after their ejection from the ocean, the relative molar contributions of monosaccharides to CCHO were compared between the bulk and SML from the leads/polynyas, MIZ, ice-free ocean and melt pond samples, as well as the sub-and supermicron aerosol particles and fog water (**Figure 8**). The composition of marine carbohydrates in seawater strongly depends on the dominating microbial species, season, diagenetic state, availability of nutrients and environmental stress factors (Engbrodt, 2001; Goldberg et al., 2011) leading to a natural variability among individual samples even within small spatial scales. Consequently, to enable the direct comparison of seawater with atmospheric samples of this field study with an elevated level of statistical certainty, here we compare the mean values of the entire data set, instead of individual samples. Finally, in addition to the changes of the monosaccharide patterns of CCHO, the systematic degradation of CCHO to dFCHO was observed in the atmosphere and will be discussed within this section.

CCHO composition in different sea-ice-related sea surface compartments and depths is similar. In seawater (bulk and SML), glucose (means= 35–48 mol%), galactose (means= 13–18 mol%) and xylose (means= 7–16 mol%) dominated the CCHO composition followed by smaller contributions of other neutral sugars, amino sugars, uronic acids and muramic acid (**Figure 8**). Considering the natural variability among individual samples, there were no significant differences in means between the bulk and SML, nor between the lead/polynya, MIZ, ice-free ocean and melt pond samples. Variations were observed between the dissolved and particulate fractions (**Figure SI 3**), nevertheless the combined carbohydrates within all sea-ice-related sea surface compartments followed the same pattern of the predominance of glucose, galactose and xylose. Overall, the relative monosaccharide compositions of glucose **>** (galactose ≈ xylose) **>** other (neutral or charged) monosaccharides of the seawater samples from this Arctic study appear similar to the monosaccharide compositions investigated in the SML and bulk water from the Central Arctic Ocean (Gao et al., 2012) and at the western Antarctic peninsula (Zeppenfeld et al., 2021a), the meltwater of Arctic multiyear sea ice (Amon et al., 2001) and the epipelagic water from the Ross Sea (Kirchman et al., 2001).

Less galactose, but more muramic acid in atmospheric CCHO_{aer} and CCHO_{fog}. Atmospheric samples showed a different monosaccharide pattern within the hydrolyzed CCHO in comparison to the seawater and melt pond samples. While glucose (means= 41 mol% for fog; 50 mol% for submicron and 60 mol% for supermicron aerosol particles) and xylose (means= 16; 15 and 15 mol%) still prevailed over the relative monosaccharide pattern, the contribution of galactose (means= 6; 3 and 3 mol%) was strongly reduced, both in fog and aerosol particles. On the other hand, the ratio of muramic acid was
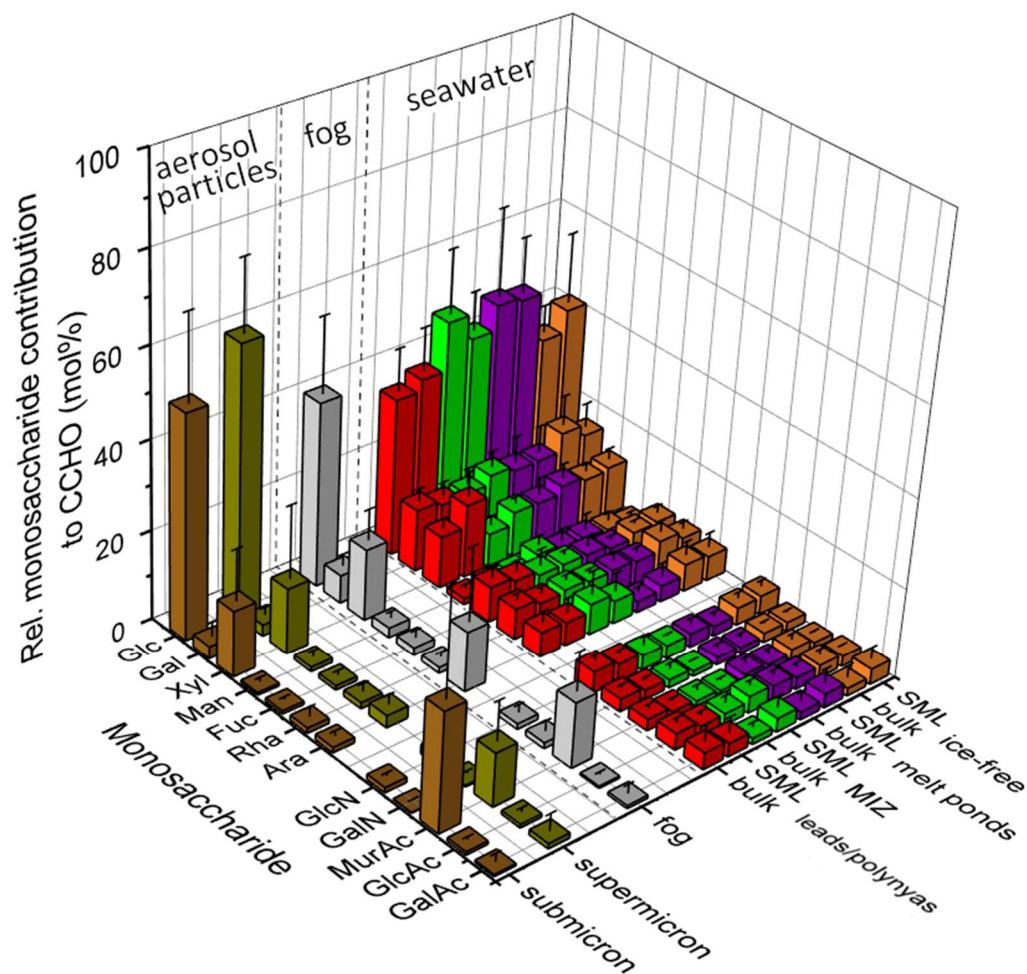
Figure 8. Relative monosaccharide composition of combined carbohydrates (CCHO) after acid hydrolysis in sub-/ supermicron aerosol particles, fog water, bulk and SML samples from the leads and polynyas within the pack ice, the MIZ, the ice-free ocean and young and aged melt ponds. The 3D bar chart shows the averages and standard deviations of the relative contributions. Glc: glucose, Gal: galactose, Xyl: xylose, Man: mannose, Fuc: fucose, Ara: arabinose, GlcN: glucosamine, GalN: galactosamine, MurAc: muramic acid, GlcAc: glucuronic acid, GalAc: galacturonic acid.

727   strongly elevated in aerosol particles (means= 12 and 26 mol%) and fog water (mean= 14 mol%) in

728   comparison to the oceanic samples (means= 0.9–2.6 mol%). These differences of the relative

729   monosaccharide contributions to CCHO among the seawater and the atmospheric samples described

730   within this study are in good agreement with the sea-air transfer investigations conducted in the

731   Southern Ocean at the western Antarctic peninsula (Zeppenfeld et al., 2021a). Consequently, the

732   occurring phenomenon might be independent from the sampling location and could be explained by

733   three possible atmospheric processes, such as (1) a chemo-selective sea-air transfer of certain oligo-

734   or polysaccharides over others, (2) an atmospheric transformation due to abiotic chemical reactions

735   or (3) an atmospheric transformation due to microbiological activities. Among these possible

736   pathways, Zeppenfeld et al. (2021) presumed the secondary atmospheric transformation caused by

737   microbiological metabolism as the most probable or at least most dominant one supported by the

738   prevalence of muramic acid, an amino sugar acid naturally occurring in bacterial cell walls (Mimura

739   and Romano, 1985; Sud and Tyler, 1964), and the very selective absence of certain monosaccharides

740   in the $CCHO_{aer}$ in aerosol particles as it was observed in this Arctic study as well.

741   ***Formation of combined arabinose in fog.*** A comparison of the monosaccharide composition of aerosol

742   particles and fog water showed great similarity regarding dominant contributions from glucose, xylose

743   and muramic acid. It seems plausible that the fog water droplets contained the same inorganic and

744   organic compounds found in the SSA particles assuming that SSA particles activated the formation of

745   fog droplets as CCN due to their rather large diameters and high hygroscopicity. Apart from that,

746   however, a significant difference was observed in the increased relative contribution of arabinose in

747   fog (mean= 13 mol%) compared to aerosol particles (means= 1.2 and 2.7 mol%) indicating a formation

748   of arabinose in the liquid phase. During a marine microcosm experiment performed by Hasenecz et al.

749   (2020), a strong link was observed between the release of arabinose-containing polysaccharides in

750   form of EPS and the presence of heterotrophic bacteria and stressed phytoplankton. Furthermore, a

751   strain of the psychrotolerant marine bacterium *Pseudoalteromonas* sp. has been shown to produce

752   EPS mainly composed from glucose, arabinose and xylose (Casillo et al., 2018; Qin et al., 2007).

753   Consequently, the release of arabinose-containing EPS in fog could be a plausible protection

754   mechanism of microorganisms contained within a droplet against freezing damage under low Arctic

755   temperatures.

756   ***Indication for microbial activities in the atmosphere.*** Intact bacterial cells at atmospheric

757   concentrations between 5×10^2 and 8×10^4 cells m^{-3} for remote marine and ice-covered regions (Šantl-

758   Temkiv et al., 2018; Mayol et al., 2017), cell-bound and free enzymes have been detected in ambient

759   and nascent marine super- and submicron aerosol particles during several field and tank studies (Aller

760   et al., 2005; Hasenecz et al., 2020; Malfatti et al., 2019; Marks et al., 2001; Rastelli et al., 2017; Šantl-

761   Temkiv et al., 2020; Uetake et al., 2020). For surviving in this hostile environment, some of these

762   microbes have developed a remarkable resilience towards extreme environmental stressors, such as

763   high UV radiation, radical exposure, changing osmolarity, freezing temperatures and desiccation. As

764   survival strategies could serve the selective enzymatic consumption of airborne labile carbohydrates

765   explaining the here observed loss of galactose and the persistence of xylose, the release of protecting

766   biofilms from EPS, carotenoid pigmentation or the formation of own precipitating hydrometeors by

767   enabling condensation on a surface as a CCN or freezing by IN active surfaces to reduce their

768   atmospheric residence time (Delort et al., 2010; Matulová et al., 2014; Šantl-Temkiv et al., 2020).

769   Consequently, an enzymatic transformation might serve as a plausible explanation for the selective

770   removal of certain monosaccharides within $CCHO_{aer}$ and $CCHO_{fog}$ observed here. However, the survival

771   and the metabolic activity of microorganisms is restricted by the presence of water (Ervens and Amato,

772   2020; Haddrell and Thomas, 2017) identifying liquid hydrometeors or fresh SSA as the most biologically

773 active atmospheric hotspots. In contrast to most of the ambient aerosol particles, fog droplets provide

774 enough water essential for bacterial activities. However, they might freeze under Arctic sub-zero

775 temperatures possibly causing damage to the microbial cells, which might explain an in-situ formation

776 of a protecting biofilm from arabinose-containing EPS. In a previous Arctic study, Orellana et al. (2011)

777 readily detected microgels in aerosol particles, cloud and fog water most likely emitted from the

778 surface water and the SML via bubble bursting. Indications for an in-situ generation of marine

779 microgels in fog water as an additional source to the primary release from the ocean by bubble bursting

780 have been observed by van Pinxteren et al. (2022) in the tropical Atlantic Ocean.

781 The selective sea-air transfer of certain carbohydrates over others and the abiotic degradation as

782 further possible pathways to the biotic transformation of marine $CCHO_{aer}$ have been discussed in detail

783 in Zeppenfeld et al. (2021), but do not appear, based on the current state of knowledge, as likely

784 explanations of the very selective CCHO degradation and formation of other CCHO observed here.

785 More future lab and mesocosm experiments are required to elucidate the contribution of each of these

786 processes. Finally, the similarity between the carbohydrate compositions of fog water and aerosol

787 particles, both two atmospheric compartments collected with different instrumentation, allows to rule

788 out artefacts of the different sampling and extraction techniques as a reason for the observed

789 differences to the seawater.

790 ***Depolymerization of CCHO to dFCHO, seawater versus atmosphere.*** Free glucose, by far the most

791 prevailing monosaccharide among dFCHO in seawater, ranged between 0.6 and 51 µg L^{-1} during the

792 PS106 cruise in the bulk and the SML (Zeppenfeld et al., 2019a). Thus, dFCHO/CHO ratios, meaning the

793 contribution of sugar monomers to all marine carbohydrates measured in this study, varied between

794 1–14% with an average of 5±3%. Conversely, 86–99% (mean: 95±3) of carbohydrates in the bulk and

795 SML of ocean seawater and melt ponds were incorporated into an oligo- or polysaccharidic structure.

796 CCHO can be hydrolyzed to dFCHO either in an acidic environment or enzymatically by heterotrophic

797 bacteria (Arnosti, 2000; Panagiotopoulos and Sempéré, 2005). Seawater from the Arctic Ocean is

798 slightly alkaline with reported pH values between 7.98 and 8.49 (Rérolle et al., 2016; Tynan et al.,

799 2016), while the pH of melt pond water has been observed to be more variable from mildly acidic (6.1)

800 to more alkaline (10.8) (Bates et al., 2014). In agreement with previous findings, the oceanic surface

801 seawater (pH: 7.98–8.66), including the samples from the MIZ, ice-free ocean and open

802 leads/polynyas, and the melt pond samples (pH: 7.26–8.62) were slightly alkaline in this study.

803 Consequently, it is more plausible that the depolymerization of CCHO in seawater can be ascribed to

804 bacterial activities rather than acid hydrolysis. Since dFCHO are readily resorbed by heterotrophic

805 bacteria with high turnover rates (Ittekkot et al., 1981; Kirchman et al., 2001), concentrations of these

806 monosaccharides are rather low in seawater.

In contrast, in aerosol particles, higher dFCHO/CHO ratios up to 35% occurred in some selected samples, which is much higher than in seawater, suggesting that CCHO might be depolymerized in the atmosphere. SSA particles are known to significantly acidify within minutes after their release due to the uptake of acidic gases, atmospheric aging reactions with sulfuric dioxide and water loss (Angle et al., 2021). In this context, the surface-to-volume ratio determines the efficiency of the acidification effect, which means that it is most pronounced for submicron SSA particles with reported pH values of 1.5–2.6 within a few minutes in a tank study (Angle et al., 2021), and less pronounced for supermicron SSA particles or cloud droplets (Angle et al., 2022). Consequently, it is conceivable that an acid hydrolysis of CCHO$_{aer}$ to monomeric dFCHO$_{aer}$ occurs at the surface or within the bulk of SSA particles leading to quick atmospheric aging. However, due to analytical constraints, such as the limits of detections (LODs) of the methodology, the dFCHO in size-resolved aerosol particles could not be detected in all samples and the data availability is not strong enough to draw more conclusions for aerosol particles.

In fog, where LODs did not represent an issue due to the high concentrations, dFCHO/CHO ratios exceeding those in seawater were also observed, ranging from 1-60% (mean: 27±16%). The monosaccharide composition of dFCHO$_{fog}$ was primarily made up of glucose, arabinose, fructose, and xylose, with minor contributions from glucosamine, galactose, mannose, rhamnose, and fucose. While dFCHO$_{fog}$ and CCHO$_{fog}$ shared similar dominant monosaccharides, fructose was only present in dFCHO$_{fog}$. This absence in CCHO$_{fog}$ is attributed to fructose's low stability during the analytical preparation for CCHO analysis (Panagiotopoulos and Sempéré, 2005). As a result, fructose won't be further discussed. In this study, pH values of fog water ranged between 5.7 and 6.8, which is 1–2 magnitudes more acidic than in seawater. Polysaccharides are known to depolymerize due to acid hydrolysis, especially at elevated temperatures. The pH-stability can be largely variable among the different polysaccharides; however, we are not aware of studies that have shown such fast depolymerizations, in the sense of time scales relevant for atmospheric lifetime of aerosol particles, at such mildly acid conditions and low temperatures as those of the Arctic atmosphere. Furthermore, there was no significant correlation between the pH and the dFCHO/CHO of these cloud samples. Consequently, there are no indications that the majority of CCHO was hydrolyzed inside the cloud droplets, however it might be conceivable that hydrolysis had readily occurred within the non-activated SSA particle where pH values were much lower.

Besides an acid hydrolysis induced by quick atmospheric acidification of SSA particles, atmospheric radicals, such as OH (Trueblood et al., 2019), or photolytic cleavages of glycosidic bonds (Kubota et al., 1976) could have contributed to the degradation of atmospheric CCHO to monomeric dFCHO in SSA and marine fog. For these processes, however, still hardly any systematic lab studies have been

conducted for the plurality of marine polysaccharides, which makes a classification of the meaning of these processes difficult. A preferred sea-air transfer of dFCHO over CCHO to explain this observation seems unlikely based on the missing enrichment of neutral dFCHO in contrast to the high EF_{aer} of CCHO shown in tank studies (Hasenecz et al., 2019, 2020). Finally, a microbial depolymerization of CCHO by extracellular enzymes in fog cannot be entirely ruled out considering that the activity of some polysaccharide-degrading enzymes, such as α- and β-glucosidase, have been found to accelerate in seawater with increasing acidity (Piontek et al., 2010). However, this finding was conducted for a pH range only 0.3 pH units lower than the typical pH of seawater and it is not sure, if this finding can be transferred to the more acid conditions in aerosol particles and fog water.

Several aging processes in the atmosphere. We observed significant changes between the chemical composition of marine carbohydrates in the surface seawater, including the bulk and SML, and atmospheric carbohydrates, including aerosol particles and fog. Based on the changing monosaccharide composition pattern of CCHO with selective degradation and formation of specific monosaccharides within CCHO, we conclude microbial or enzymatic activities within the aerosol particles of fog droplets. Furthermore, the increasing contribution of dFCHO to the total carbohydrate pool in fog and aerosol particles might be attributed to a hydrolytic cleavage of the glycosidic linkages between monosaccharide unites within the oligo-and polysaccharides after a quick atmospheric acidification of SSA particles. Consequently, atmospheric carbohydrates experience quick atmospheric aging, potentially due to both biological and abiotic processes, after their release from the ocean. Possibly, this could affect the CCN and INP properties of marine carbohydrates and hence the formation and properties of clouds.

3.6 Perspective assessment of CCHO via bio-optical parameters

The absorption of phytoplankton (a_{ph}) and CDOM (a_{CDOM}) are bio-optical parameters providing additional information about the chemical and microbiological history of the water masses within the particulate and dissolved phase, respectively. They can be measured on discrete water samples and can also be assessed as products from satellites (Lefering et al., 2017; Matsuoka et al., 2012, 2013; Röttgers et al., 2016). Here we tested, if a_{ph} or CDOM parameters correlate with CCHO in seawater to potentially enable the remote-sensing approximation of marine CCHO in seawater and potentially in the atmosphere.

Good assessment of CCHO in seawater via a_{ph}440. a_{ph}440 derived from the phytoplankton absorption spectrum is directly related to the biomarker TChl-*a* indicating phytoplankton biomass (Bricaud et al., 2004; Phongphattarawat, 2016). The advantage of using a_{ph}440 over pigment data, including TChl-*a* from full high-performance liquid chromatography (HPLC) analysis (e.g. Barlow et al., 1997; Taylor et al., 2011), is the lower need of sample volume for the analysis. This allows the determination of values in the SML samples as well (Zäncker et al., 2017), which are laborious to collect and therefore limited in availability. In this study, a_{ph}440 strongly correlated with *p*CCHO (R=0.90, p<0.001) in bulk and SML samples (**Figure 9a**) showing a direct link with fresh phytoplankton biomass production. A similar link has been described before for TChl-*a* and *p*CCHO in the photic layer of the Ross Sea (Fabiano et al., 1993), in the ocean west of the Antarctic peninsula (Zeppenfeld et al., 2021a) and between TChl-*a* and the particulate form of laminarin, an algal polysaccharide, in Arctic and Atlantic water samples (Becker et al., 2020). *d*CCHO showed a good, but weaker correlation with a_{ph}440 (R=0.66, p<0.001) than *p*CCHO. This finding supports the assumption that *p*CCHO are rather freshly produced by local autotrophs, while the link between *d*CCHO with their primary production was already obscured by subsequent transformation processes resulting in a more recalcitrant, long-lived mix of macromolecules (Goldberg et al., 2011; Hansell, 2013; Keene et al., 2017). Nevertheless, CCHO, the sum from *d*CCHO and *p*CCHO, showed a high correlation with a_{ph}440 (R=0.84, p<0.001, **Figure 9b**) leading to the conclusion that this bio-optical parameter derived from the $a_{ph}(\lambda)$ spectrum is suitable to assess the total amount of CCHO in the surface seawater of the different sea-ice-related sea surface compartments of the Arctic.

Good assessment of CCHO in seawater via a_{CDOM}350. In this study, high correlations were observed between *d*CCHO and a_{CDOM}350 (R=0.66, p<0.001, **Figure 10a**), and weaker correlations between *d*CCHO and a_{CDOM}443 (R=0.53, p<0.001, **Figure 10b**). The better correlation at λ=350 nm compared to 443 nm can be explained by the fact that a_{CDOM} exponentially decreases with wavelength. While absorption by CDOM is higher at λ=350 nm, it is much closer to the method detection limit at λ=443 nm and is

895 therefore more error-prone. However, with current satellite products only a_{CDOM} at 440 nm can be
896 retrieved.

897 Previous studies reported strong correlations between a_{CDOM}350 and dissolved organic carbon (DOC)
898 in Arctic seawater (Gonçalves-Araujo et al., 2015; Spencer et al., 2009; Stedmon et al., 2011; Walker
899 et al., 2013). Consequently, it is conceivable that *d*CCHO, an important constituent of DOC, shows good
900 correlations as well. Surprisingly, the correlation between CCHO (sum of *d*CCHO and *p*CCHO) and
901 a_{CDOM}350 was strongest (R=0.85, p<0.001, **Figure 10c**), indicating that CDOM retrieval from high-
902 resolution satellite data could allow a good approximation of CCHO in Arctic seawater.

903
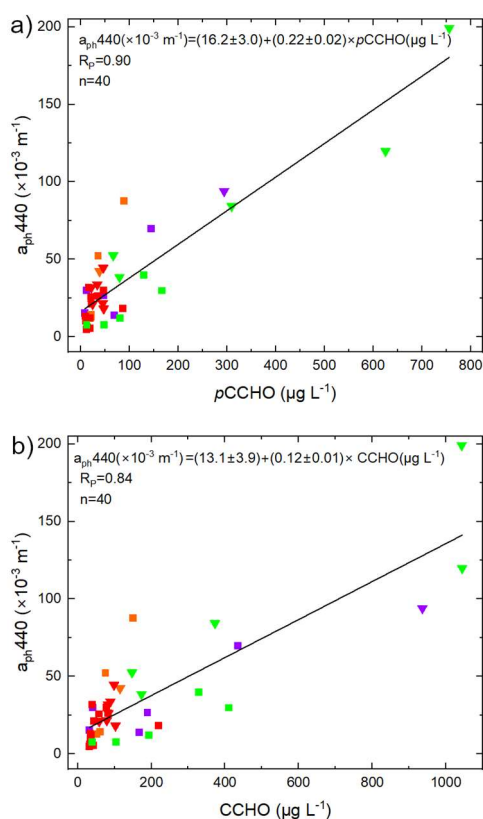
Figure 9. Correlation plots of a_{ph}440 derived from PAB spectra against a) *p*CCHO and b) CCHO. Triangles: SML, squares: bulk. Green: marginal ice zone (MIZ), purple: melt ponds, orange: ice-free ocean, red: open leads/polynyas in the pack ice.

918

919

920

921

922

923
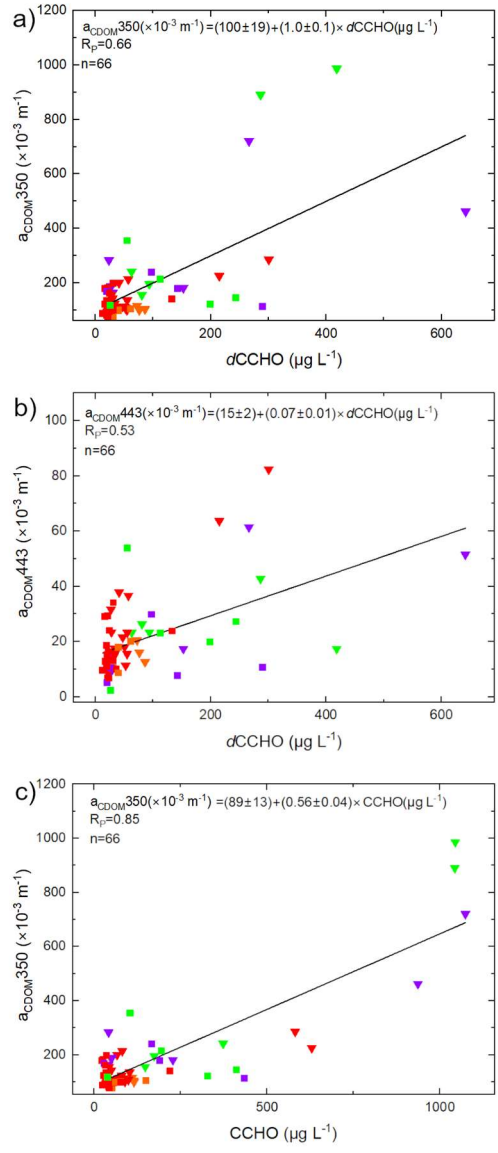
Figure 10. Correlation plots of a) $a_{CDOM}350$ against dCCHO, b) $a_{CDOM}443$ against dCCHO and c) $a_{CDOM}350$ against CCHO. Triangles: SML, squares: bulk. Green: marginal ice zone (MIZ), purple: melt ponds, orange: ice-free ocean, red: open leads/polynyas in the pack ice.

4. Summary and Atmospheric Implications

943 We studied the sea-air transfer of marine carbohydrates from field samples collected in the Arctic
944 during the PS106 campaign from May to July 2017. Large differences of absolute CCHO concentrations
945 and SML enrichments were observed among the different sea-ice-related sea surface compartments
946 (leads/polynyas within the pack ice, ice-free ocean, MIZ, melt ponds). $CCHO_{aer}$ were detected in the
947 sub- and supermicron aerosol particles with indications for primary emissions from the sea through
948 bubble bursting, though the correlations with the SSA tracer Na^+ and wind speed were possibly
949 reduced due to the presence of sea ice influencing the wind-induced SSA emission mechanisms.
950 Atmospheric CCHO and Na^+ concentrations in fog strongly exceeded those of the aerosol particles likely
951 due to a physical phenomenon. Large enrichments of CCHO in aerosol and fog compared to bulk
952 seawater were observed. The extent of these enrichments varied based on the type of sea-ice-related
953 sea surface compartment assumed as the oceanic source for atmospheric CCHO. We observed a
954 subsequent atmospheric aging of CCHO in the atmosphere, both in aerosol particles and fog, noticed
955 by the selective loss and formation of certain monosaccharide units within CCHO suggesting selective
956 enzymatic/microbial activities, and a depolymerization of CCHO to dFCHO, most measurable in fog
957 water and likely due to abiotic degradation, e.g. acid hydrolysis. CCHO correlated well with bio-optical
958 parameters, such as $a_{ph}440$ from phytoplankton absorption and $a_{CDOM}350$. These parameters can be
959 measured via remote sensing and may allow the retrieval of CCHO from satellite data, which
960 potentially will enable an accurate modelling of atmospheric CCHO concentrations as soon as all
961 emission and atmospheric aging processes are sufficiently understood. This study shows that the Arctic
962 is a complex environment, where the diversity of sea-ice-related sea surface compartments needs to
963 be considered as primary sources of marine CCHO or other organic compounds, and where these
964 molecules can be transformed after their primary sea-air transfer by biological and abiotic processes
965 in the atmosphere.

966 Marine carbohydrates are assumed to impact cloud properties by acting as CCN and INP (Alpert et al.
967 2022; Leck et al., 2013; Orellana et al., 2011; van Pinxteren et al., 2022). Studying the chemical identity
968 of those atmospheric nucleation particles, their emission mechanisms and their transformation due to
969 atmospheric aging can strongly improve the understanding of the cloud formation in the Arctic, cloud
970 microphysical properties, the radiation budget, cryosphere-ocean-atmosphere interactions and
971 eventually feedback mechanisms in the frame of Arctic amplification. It can be assumed that within
972 the warming Arctic, where sea ice extent is continuously shrinking, the MIZ area will expand (Strong
973 and Rigor, 2013) and the number of biologically-active melt ponds will increase during the summer
974 season in the next years. These new MIZ regions and melt ponds could potentially produce more
975 marine carbohydrates than the ice-free ocean or open leads within the pack ice leading to enhanced

976 CCN and INP populations in the Arctic atmosphere serving as a still not well-explored feedback
977 mechanism within Arctic amplification.

978 ***Data availability.*** All data are available on the public repository PANGAEA:
979 https://doi.org/10.1594/PANGAEA.962208 and https://doi.org/10.1594/PANGAEA.932573 (for fog
980 samples); https://doi.org/10.1594/PANGAEA.962210 and https://doi.org/10.1594/PANGAEA.932569
981 (for aerosol particles); https://doi.org/10.1594/PANGAEA.961004 (for seawater samples).

982 ***Author contribution.*** SZ wrote the manuscript with contributions from MvP, MH, MZ, AB and HH. SZ,
983 MvP and MH collected the field samples during the PS106 campaign. SZ performed the laboratory
984 carbohydrate analysis and statistical evaluation. MZ and AB assessed the bio-optical parameters. All
985 co-authors proofread and commented the manuscript.

986 ***Competing interests.*** The authors declare that they have no conflict of interest.

987 ***Acknowledgements.*** We gratefully acknowledge the funding by the Deutsche Forschungsgemeinschaft
988 (DFG, German Research Foundation, Projektnummer 268020496−TRR 172) within the Transregional
989 Collaborative Research Center "ArctiC Amplification: Climate Relevant Atmospheric and SurfaCe
990 Processes, and Feedback Mechanisms (AC)[3]". This research has been supported by the DFG SPP 1158,
991 grant number 424326801 by enabling the access to melt pond data. We thank Andreas Macke and
992 Hauke Flores, chief scientists for the RV *Polarstern* cruises PS106.1 and PS106.2 (expedition grant
993 number AWI_PS106_00), and the captain and the crew of RV *Polarstern* for their support during the
994 expedition from May to July 2017. We thank Andrea Haudek and Hartmut Haudek for the development
995 and construction of the conditioning tube and the wind control system connected to the Berner
996 impactor. We thank Anett Dietze, Susanne Fuchs and Anke Rödger for the mass, inorganic ion and
997 OC/EC measurements. We acknowledge René Rabe and Sonja Wiegmann for supporting the
998 preparation of PS106 chemical equipment and optical instrumentation, respectively, and Yangyang Liu
999 for introducing the optical measurement procedure before PS106.

1000 ***Financial support.*** This research has been supported by the Deutsche Forschungsgemeinschaft (DFG,
1001 German Research Foundation, Projektnummer 268020496−TRR 172) within the Transregional
1002 Collaborative Research Center "ArctiC Amplification: Climate Relevant Atmospheric and SurfaCe
1003 Processes, and Feedback Mechanisms (AC)[3]" in subprojects B04 and C03.

1004 **List of abbreviations**

1005 a_{CDOM} absorption coefficient by colored dissolved organic carbon
1006 aer   aerosol particles
1007 a_{NAP} absorption coefficient by non-algal particles
1008 ANOVA   Analysis of Variance
1009 a_p absorption coefficient by total particles
1010 a_{ph} absorption coefficient by phytoplankton

1011	Ara	arabinose
1012	atmos	atmospheric concentrations
1013	C-CCHO	carbon contained within the combined carbohydrate
1014	CCHO	combined carbohydrates
1015	CCN	cloud condensation nuclei
1016	CDOM	colored dissolved organic matter
1017	CHO	carbohydrates
1018	*d*CCHO	dissolved combined carbohydrates
1019	*d*FCHO	dissolved free carbohydrates
1020	EF	enrichment factor
1021	EPS	exopolymeric substances
1022	ERDDAP	Environmental Research Division's Data Access Program
1023	FAA	free amino acids
1024	Fru	fructose
1025	Fuc	fucose
1026	Gal	galactose
1027	GalN	galactosamine
1028	GalAc	galacturonic acid
1029	Glc	glucose
1030	GlcAc	glucuronic acid
1031	GlcN	glucosamine
1032	HPAEC-PAD	high-performance anion-exchange chromatography with pulsed amperometric detection
1033	HPLC	high-performance liquid chromatography
1034	INP	ice nucleating particles
1035	LWCC	liquid waveguide capillary cell
1036	Man	mannose
1037	MIZ	marginal ice zone
1038	MurAc	muramic acid
1039	Na^+	sodium ion
1040	NOAA	National Oceanic and Atmospheric Administration
1041	OC	organic carbon
1042	OM	organic matter
1043	PAB	particulate absorption
1044	*p*CCHO	particulate combined carbohydrates
1045	PM	particulate matter
1046	Rha	rhamnose
1047	SML	sea surface microlayer
1048	SSA	sea spray aerosol
1049	sub	submicron
1050	super	supermicron
1051	TChl-*a*	total chlorophyll *a*
1052	TEP	transparent exopolymer particles
1053	QFT-ICAM	quantitative filtration technique with an integrative-cavity absorption meter setup
1054	Xyl	xylose

References

Alderkamp, A.-C., Buma, A. G. J., and van Rijssel, M.: The carbohydrates of Phaeocystis and their degradation in the microbial food web, Biogeochemistry, 83, 99–118, https://doi.org/10.1007/s10533-007-9078-2, 2007.

Aller, J. Y., Kuznetsova, M. R., Jahns, C. J., and Kemp, P. F.: The sea surface microlayer as a source of viral and bacterial enrichment in marine aerosols, Journal of Aerosol Science, 36, 801–812, https://doi.org/10.1016/j.jaerosci.2004.10.012, 2005.

Aller, J. Y., Radway, J. C., Kilthau, W. P., Bothe, D. W., Wilson, T. W., Vaillancourt, R. D., Quinn, P. K., Coffman, D. J., Murray, B. J., and Knopf, D. A.: Size-resolved characterization of the polysaccharidic and proteinaceous components of sea spray aerosol, Atmospheric Environment, 154, 331–347, https://doi.org/10.1016/j.atmosenv.2017.01.053, 2017.

Alpert, P. A., Kilthau, W. P., O'Brien, R. E., Moffet, R. C., Gilles, M. K., Wang, B., Laskin, A., Aller, J. Y., and Knopf, D. A.: Ice-nucleating agents in sea spray aerosol identified and quantified with a holistic multimodal freezing model, Science Advances, 8, eabq6842, https://doi.org/10.1126/sciadv.abq6842, 2022.

Álvarez, E., Losa, S. N., Bracher, A., Thoms, S., and Völker, C.: Phytoplankton Light Absorption Impacted by Photoprotective Carotenoids in a Global Ocean Spectrally-Resolved Biogeochemistry Model, Journal of Advances in Modeling Earth Systems, 14, e2022MS003126, https://doi.org/10.1029/2022MS003126, 2022.

Amon, R. M. W., Fitznar, H.-P., and Benner, R.: Linkages among the bioreactivity, chemical composition, and diagenetic state of marine dissolved organic matter, Limnology and Oceanography, 46, 287–297, 2001.

Angle, K., Grassian, V. H., and Ault, A. P.: The rapid acidification of sea spray aerosols, Physics today, 75, https://doi.org/10.1063/PT.3.4926, 2022.

Angle, K. J., Crocker, D. R., Simpson, R. M. C., Mayer, K. J., Garofalo, L. A., Moore, A. N., Garcia, S. L. M., Or, V. W., Srinivasan, S., Farhan, M., Sauer, J. S., Lee, C., Pothier, M. A., Farmer, D. K., Martz, T. R., Bertram, T. H., Cappa, C. D., Prather, K. A., and Grassian, V. H.: Acidity across the interface from the ocean surface to sea spray aerosol, PNAS, 118, https://doi.org/10.1073/pnas.2018397118, 2021.

Arnosti, C.: Substrate specificity in polysaccharide hydrolysis: Contrasts between bottom water and sediments, Limnology and Oceanography, 45, 1112–1119, https://doi.org/10.4319/lo.2000.45.5.1112, 2000.

Aslam, S. N., Michel, C., Niemi, A., and Underwood, G. J. C.: Patterns and drivers of carbohydrate budgets in ice algal assemblages from first year Arctic sea ice, Limnology and Oceanography, 61, 919–937, https://doi.org/10.1002/lno.10260, 2016.

Azetsu-Scott, K. and Passow, U.: Ascending marine particles: Significance of transparent exopolymer particles (TEP) in the upper ocean, Limnology and Oceanography, 49, 741–748, https://doi.org/10.4319/lo.2004.49.3.0741, 2004.

Barlow, R., Cummings, D., and Gibb, S.: Improved resolution of mono- and divinyl chlorophylls a and b and zeaxanthin and lutein in phytoplankton extracts using reverse phase C-8 HPLC, Marine Ecology Progress Series, 161, 303–307, https://doi.org/10.3354/meps161303, 1997.

Barthel, S., Tegen, I., and Wolke, R.: Do new sea spray aerosol source functions improve the results of a regional aerosol model?, Atmospheric Environment, 198, 265–278, https://doi.org/10.1016/j.atmosenv.2018.10.016, 2019.

Bates, N. R., Garley, R., Frey, K. E., Shake, K. L., and Mathis, J. T.: Sea-ice melt CO_2–carbonate chemistry in the western Arctic Ocean: meltwater contributions to air–sea CO_2 gas exchange, mixed-layer properties and rates of net community production under sea ice, Biogeosciences, 11, 6769–6789, https://doi.org/10.5194/bg-11-6769-2014, 2014.

Becker, S., Tebben, J., Coffinet, S., Wiltshire, K., Iversen, M. H., Harder, T., Hinrichs, K.-U., and Hehemann, J.-H.: Laminarin is a major molecule in the marine carbon cycle, PNAS, 117, 6599–6607, https://doi.org/10.1073/pnas.1917001117, 2020.

Benner, R. and Kaiser, K.: Abundance of amino sugars and peptidoglycan in marine particulate and dissolved organic matter, Limnology and Oceanography, 48, 118–128, https://doi.org/10.4319/lo.2003.48.1.0118, 2003.

Bigg, E. K. and Leck, C.: The composition of fragments of bubbles bursting at the ocean surface, Journal of Geophysical Research: Atmospheres, 113, https://doi.org/10.1029/2007JD009078, 2008.

Bikerman, J. J.: Foams, Springer Science & Business Media, 344 pp., 2013.

Bozem, H., Hoor, P., Kunkel, D., Köllner, F., Schneider, J., Herber, A., Schulz, H., Leaitch, W. R., Aliabadi, A. A., Willis, M. D., Burkart, J., and Abbatt, J. P. D.: Characterization of transport regimes and the polar dome during Arctic spring and summer using in situ aircraft measurements, Atmospheric Chemistry and Physics, 19, 15049–15071, https://doi.org/10.5194/acp-19-15049-2019, 2019.

Bricaud, A., Claustre, H., Ras, J., and Oubelkheir, K.: Natural variability of phytoplanktonic absorption in oceanic waters: Influence of the size structure of algal populations, Journal of Geophysical Research: Oceans, 109, https://doi.org/10.1029/2004JC002419, 2004.

1107 Burrows, S. M., Ogunro, O., Frossard, A., Russell, L. M., Rasch, P. J., and Elliott, S.: A Physically Based Framework for Modelling
1108 the Organic Fractionation of Sea Spray Aerosol from Bubble Film Langmuir Equilibria, Atmospheric Chemistry and Physics,
1109 14(24):13601–13629, https://doi.org/10.5194/acp-14-13601-2014, 2014.

1110 Burrows, S. M., Gobrogge, E., Fu, L., Link, K., Elliott, S. M., Wang, H., and Walker, R.: OCEANFILMS-2: Representing
1111 coadsorption of saccharides in marine films and potential impacts on modeled marine aerosol chemistry, Geophysical
1112 Research Letters, 43, 8306–8313, https://doi.org/10.1002/2016GL069070, 2016.

1113 Callaghan, A. H., Deane, G. B., Stokes, M. D., and Ward, B.: Observed variation in the decay time of oceanic whitecap foam,
1114 Journal of Geophysical Research: Oceans, 117, https://doi.org/10.1029/2012JC008147, 2012.

1115 Casillo, A., Lanzetta, R., Parrilli, M., and Corsaro, M. M.: Exopolysaccharides from Marine and Marine Extremophilic Bacteria:
1116 Structures, Properties, Ecological Roles and Applications, Marine Drugs, 16, 69, https://doi.org/10.3390/md16020069, 2018.

1117 Chen, Q., Mirrielees, J. A., Thanekar, S., Loeb, N. A., Kirpes, R. M., Upchurch, L. M., Barget, A. J., Lata, N. N., Raso, A. R. W.,
1118 McNamara, S. M., China, S., Quinn, P. K., Ault, A. P., Kennedy, A., Shepson, P. B., Fuentes, J. D., and Pratt, K. A.: Atmospheric
1119 particle abundance and sea salt aerosol observations in the springtime Arctic: a focus on blowing snow and leads,
1120 Atmospheric Chemistry and Physics, 22, 15263–15285, https://doi.org/10.5194/acp-22-15263-2022, 2022.

1121 Chi, J. W., Li, W. J., Zhang, D. Z., Zhang, J. C., Lin, Y. T., Shen, X. J., Sun, J. Y., Chen, J. M., Zhang, X. Y., Zhang, Y. M., and Wang,
1122 W. X.: Sea salt aerosols as a reactive surface for inorganic and organic acidic gases in the Arctic troposphere, Atmospheric
1123 Chemistry and Physics, 15, 11341–11353, https://doi.org/10.5194/acp-15-11341-2015, 2015.

1124 Creamean, J. M., Barry, K., Hill, T. C. J., Hume, C., DeMott, P. J., Shupe, M. D., Dahlke, S., Willmes, S., Schmale, J., Beck, I.,
1125 Hoppe, C. J. M., Fong, A., Chamberlain, E., Bowman, J., Scharien, R., and Persson, O.: Annual cycle observations of aerosols
1126 capable of ice formation in central Arctic clouds, Nat Commun, 13, 3537, https://doi.org/10.1038/s41467-022-31182-x, 2022.

1127 Cunliffe, M., Engel, A., Frka, S., Gašparović, B., Guitart, C., Murrell, J. C., Salter, M., Stolle, C., Upstill-Goddard, R., and Wurl,
1128 O.: Sea surface microlayers: A unified physicochemical and biological perspective of the air–ocean interface, Progress in
1129 Oceanography, 109, 104–116, https://doi.org/10.1016/j.pocean.2012.08.004, 2013.

1130 Cunliffe, M. and Wurl, O.: Guide to best practices to study the ocean's surface., Marine Biological Association of the United
1131 Kingdom for SCOR, 2014.

1132 Delort, A.-M., Vaïtilingom, M., Amato, P., Sancelme, M., Parazols, M., Mailhot, G., Laj, P., and Deguillaume, L.: A short
1133 overview of the microbial population in clouds: Potential roles in atmospheric chemistry and nucleation processes,
1134 Atmospheric Research, 98, 249–260, https://doi.org/10.1016/j.atmosres.2010.07.004, 2010.

1135 DeMott, P. J., Hill, T. C. J., McCluskey, C. S., Prather, K. A., Collins, D. B., Sullivan, R. C., Ruppel, M. J., Mason, R. H., Irish, V. E.,
1136 Lee, T., Hwang, C. Y., Rhee, T. S., Snider, J. R., McMeeking, G. R., Dhaniyala, S., Lewis, E. R., Wentzell, J. J. B., Abbatt, J., Lee,
1137 C., Sultana, C. M., Ault, A. P., Axson, J. L., Martinez, M. D., Venero, I., Santos-Figueroa, G., Stokes, M. D., Deane, G. B., Mayol-
1138 Bracero, O. L., Grassian, V. H., Bertram, T. H., Bertram, A. K., Moffett, B. F., and Franc, G. D.: Sea spray aerosol as a unique
1139 source of ice nucleating particles, PNAS, 113, 5797–5803, https://doi.org/10.1073/pnas.1514034112, 2016.

1140 Demoz, B. B., Collett, J. L., and Daube, B. C.: On the Caltech Active Strand Cloudwater Collectors, Atmospheric Research, 41,
1141 47–62, https://doi.org/10.1016/0169-8095(95)00044-5, 1996.

1142 Dominutti, P. A., Renard, P., Vaïtilingom, M., Bianco, A., Baray, J.-L., Borbon, A., Bourianne, T., Burnet, F., Colomb, A., Delort,
1143 A.-M., Duflot, V., Houdier, S., Jaffrezo, J.-L., Joly, M., Leremboure, M., Metzger, J.-M., Pichon, J.-M., Ribeiro, M., Rocco, M.,
1144 Tulet, P., Vella, A., Leriche, M., and Deguillaume, L.: Insights into tropical cloud chemistry in Réunion (Indian Ocean): results
1145 from the BIO-MAÏDO campaign, Atmospheric Chemistry and Physics, 22, 505–533, https://doi.org/10.5194/acp-22-505-2022,
1146 2022.

1147 Engbrodt, R.: Biogeochemistry of dissolved carbohydrates in the Arctic, Berichte zur Polar-und Meeresforschung (Reports on
1148 Polar and Marine Research), 396, 106pp, 2001.

1149 Engel, A. and Händel, N.: A novel protocol for determining the concentration and composition of sugars in particulate and in
1150 high molecular weight dissolved organic matter (HMW-DOM) in seawater, Marine Chemistry, 127, 180–191,
1151 https://doi.org/10.1016/j.marchem.2011.09.004, 2011.

1152 Engel, A., Bange, H. W., Cunliffe, M., Burrows, S. M., Friedrichs, G., Galgani, L., Herrmann, H., Hertkorn, N., Johnson, M., Liss,
1153 P. S., Quinn, P. K., Schartau, M., Soloviev, A., Stolle, C., Upstill-Goddard, R. C., van Pinxteren, M., and Zäncker, B.: The Ocean's
1154 Vital Skin: Toward an Integrated Understanding of the Sea Surface Microlayer, Front. Mar. Sci., 4, 165,
1155 https://doi.org/10.3389/fmars.2017.00165, 2017.

1156 Ervens, B. and Amato, P.: The global impact of bacterial processes on carbon mass, Atmospheric Chemistry & Physics, 20,
1157 1777–1794, https://doi.org/10.5194/acp-20-1777-2020, 2020.

1158 Fabiano, M., Povero, P., and Danovaro, R.: Distribution and composition of particulate organic matter in the Ross Sea
1159 (Antarctica), Polar Biol, 13, 525–533, https://doi.org/10.1007/BF00236394, 1993.

Facchini, M. C., Rinaldi, M., Decesari, S., Carbone, C., Finessi, E., Mircea, M., Fuzzi, S., Ceburnis, D., Flanagan, R., Nilsson, E. D., Leeuw, G. de, Martino, M., Woeltjen, J., and O'Dowd, C. D.: Primary submicron marine aerosol dominated by insoluble organic colloids and aggregates, Geophysical Research Letters, 35, https://doi.org/10.1029/2008GL034210, 2008.

Galgani, L., Piontek, J., and Engel, A.: Biopolymers form a gelatinous microlayer at the air-sea interface when Arctic sea ice melts, Scientific Reports, 6, 29465, https://doi.org/10.1038/srep29465, 2016.

Gantt, B., Meskhidze, N., Facchini, M. C., Rinaldi, M., Ceburnis, D., and O'Dowd, C. D.: Wind speed dependent size-resolved parameterization for the organic mass fraction of sea spray aerosol, Atmospheric Chemistry and Physics, 11, 8777–8790, https://doi.org/10.5194/acp-11-8777-2011, 2011.

Gao, Q., Leck, C., Rauschenberg, C., and Matrai, P. A.: On the chemical dynamics of extracellular polysaccharides in the high Arctic surface microlayer, Ocean Science, 8, 401–418, 2012.

Gilardoni, S., Massoli, P., Giulianelli, L., Rinaldi, M., Paglione, M., Pollini, F., Lanconelli, C., Poluzzi, V., Carbone, S., Hillamo, R., Russell, L. M., Facchini, M. C., and Fuzzi, S.: Fog scavenging of organic and inorganic aerosol in the Po Valley, Atmospheric Chemistry and Physics, 14, 6967–6981, https://doi.org/10.5194/acp-14-6967-2014, 2014.

Goldberg, S. J., Carlson, C. A., Brzezinski, M., Nelson, N. B., and Siegel, D. A.: Systematic removal of neutral sugars within dissolved organic matter across ocean basins, Geophysical Research Letters, 38, https://doi.org/10.1029/2011GL048620, 2011.

Gonçalves-Araujo, R., Stedmon, C. A., Heim, B., Dubinenkov, I., Kraberg, A., Moiseev, D., and Bracher, A.: From Fresh to Marine Waters: Characterization and Fate of Dissolved Organic Matter in the Lena River Delta Region, Siberia, Frontiers in Marine Science, 2, 2015.

Gong, X., Zhang, J., Croft, B., Yang, X., Frey, M. M., Bergner, N., Chang, R. Y.-W., Creamean, J. M., Kuang, C., Martin, R. V., Ranjithkumar, A., Sedlacek, A. J., Uin, J., Willmes, S., Zawadowicz, M. A., Pierce, J. R., Shupe, M. D., Schmale, J., and Wang, J.: Arctic warming by abundant fine sea salt aerosols from blowing snow, Nat. Geosci., 16, 768–774, https://doi.org/10.1038/s41561-023-01254-8, 2023.

Grythe, H., Ström, J., Krejci, R., Quinn, P., and Stohl, A.: A review of sea-spray aerosol source functions using a large global set of sea salt aerosol concentration measurements, Atmospheric Chemistry and Physics, 14, 1277–1297, https://doi.org/10.5194/acp-14-1277-2014, 2014.

Haddrell, A. E. and Thomas, R. J.: Aerobiology: Experimental Considerations, Observations, and Future Tools, Appl. Environ. Microbiol., 83, https://doi.org/10.1128/AEM.00809-17, 2017.

Hansell, D. A.: Recalcitrant Dissolved Organic Carbon Fractions, Annual Review of Marine Science, 5, 421–445, https://doi.org/10.1146/annurev-marine-120710-100757, 2013.

Hara, K., Yamagata, S., Yamanouchi, T., Sato, K., Herber, A., Iwasaka, Y., Nagatani, M., and Nakata, H.: Mixing states of individual aerosol particles in spring Arctic troposphere during ASTAR 2000 campaign, Journal of Geophysical Research: Atmospheres, 108, https://doi.org/10.1029/2002JD002513, 2003.

Hartmann, M., Gong, X., Kecorius, S., van Pinxteren, M., Vogl, T., Welti, A., Wex, H., Zeppenfeld, S., Herrmann, H., Wiedensohler, A., and Stratmann, F.: Terrestrial or marine – indications towards the origin of ice-nucleating particles during melt season in the European Arctic up to 83.7° N, Atmospheric Chemistry and Physics, 21, 11613–11636, https://doi.org/10.5194/acp-21-11613-2021, 2021.

Hasenecz, E., Jayarathne, T., Pendergraft, M. A., Santander, M. V., Mayer, K. J., Sauer, J., Lee, C., Gibson, W. S., Kruse, S. M., Malfatti, F., Prather, K. A., and Stone, E. A.: Marine bacteria affect saccharide enrichment in sea spray aerosol during a phytoplankton bloom, ACS Earth Space Chem., 4, 1638–1649, https://doi.org/10.1021/acsearthspacechem.0c00167, 2020.

Hasenecz, E. S., Kaluarachchi, C. P., Lee, H. D., Tivanski, A. V., and Stone, E. A.: Saccharide Transfer to Sea Spray Aerosol Enhanced by Surface Activity, Calcium, and Protein Interactions, ACS Earth Space Chem., 3, 2539–2548, https://doi.org/10.1021/acsearthspacechem.9b00197, 2019.

Held, A., Brooks, I. M., Leck, C., and Tjernström, M.: On the potential contribution of open lead particle emissions to the central Arctic aerosol concentration, Atmospheric Chemistry and Physics, 11, 3093–3105, https://doi.org/10.5194/acp-11-3093-2011, 2011.

Herrmann, H., Schaefer, T., Tilgner, A., Styler, S. A., Weller, C., Teich, M., and Otto, T.: Tropospheric Aqueous-Phase Chemistry: Kinetics, Mechanisms, and Its Coupling to a Changing Gas Phase, Chem. Rev., 115, 4259–4334, https://doi.org/10.1021/cr500447k, 2015.

Hoffman, E. J. and Duce, R. A.: Factors influencing the organic carbon content of marine aerosols: A laboratory study, Journal of Geophysical Research (1896-1977), 81, 3667–3670, https://doi.org/10.1029/JC081i021p03667, 1976.

Huang, J. and Jaeglé, L.: Wintertime enhancements of sea salt aerosol in polar regions consistent with a sea ice source from blowing snow, Atmos. Chem. Phys., 17, 3699–3712, https://doi.org/10.5194/acp-17-3699-2017, 2017.

1213   Istomina, L.: Retrieval of Sea Ice Surface Melt Using OLCI Data Onboard Sentinel-3, 2020, C017-07, 2020.

1214   Ittekkot, V., Brockmann, U., Michaelis, W., and Degens, E. T.: Dissolved free and combined carbohydrates during a
1215   phytoplankton bloom in the northern North Sea, Marine Ecology Progress Series, 4, 299–305, 1981.

1216   Karl, M., Leck, C., Rad, F. M., Bäcklund, A., Lopez-Aparicio, S., and Heintzenberg, J.: New insights in sources of the sub-
1217   micrometre aerosol at Mt. Zeppelin observatory (Spitsbergen) in the year 2015, Tellus B: Chemical and Physical Meteorology,
1218   71, 1613143, https://doi.org/10.1080/16000889.2019.1613143, 2019.

1219   Kecorius, S., Vogl, T., Paasonen, P., Lampilahti, J., Rothenberg, D., Wex, H., Zeppenfeld, S., van Pinxteren, M., Hartmann, M.,
1220   Henning, S., Gong, X., Welti, A., Kulmala, M., Stratmann, F., Herrmann, H., and Wiedensohler, A.: New particle formation and
1221   its effect on cloud condensation nuclei abundance in the summer Arctic: a case study in the Fram Strait and Barents Sea,
1222   Atmospheric Chemistry and Physics, 19, 14339–14364, https://doi.org/10.5194/acp-19-14339-2019, 2019.

1223   Keene, W. C., Long, M. S., Reid, J. S., Frossard, A. A., Kieber, D. J., Maben, J. R., Russell, L. M., Kinsey, J. D., Quinn, P. K., and
1224   Bates, T. S.: Factors That Modulate Properties of Primary Marine Aerosol Generated From Ambient Seawater on Ships at Sea,
1225   Journal of Geophysical Research: Atmospheres, 122, 11,961-11,990, https://doi.org/10.1002/2017JD026872, 2017.

1226   Kirchman, D. L., Meon, B., Ducklow, H. W., Carlson, C. A., Hansell, D. A., and Steward, G. F.: Glucose fluxes and concentrations
1227   of dissolved combined neutral sugars (polysaccharides) in the Ross Sea and Polar Front Zone, Antarctica, Deep Sea Research
1228   Part II: Topical Studies in Oceanography, 48, 4179–4197, https://doi.org/10.1016/S0967-0645(01)00085-6, 2001.

1229   Kirpes, R. M., Bondy, A. L., Bonanno, D., Moffet, R. C., Wang, B., Laskin, A., Ault, A. P., and Pratt, K. A.: Secondary sulfate is
1230   internally mixed with sea spray aerosol and organic aerosol in the winter Arctic, Atmos. Chem. Phys., 18, 3937–3949,
1231   https://doi.org/10.5194/acp-18-3937-2018, 2018.

1232   Krembs, C. and Deming, J. W.: The role of exopolymers in microbial adaptation to sea ice, in: Psychrophiles: from biodiversity
1233   to biotechnology, Springer, 247–264, 2008.

1234   Krembs, C., Eicken, H., Junge, K., and Deming, J. W.: High concentrations of exopolymeric substances in Arctic winter sea ice:
1235   implications for the polar ocean carbon cycle and cryoprotection of diatoms, Deep Sea Research Part I: Oceanographic
1236   Research Papers, 49, 2163–2181, https://doi.org/10.1016/S0967-0637(02)00122-X, 2002.

1237   Kubota, H., Ogiwara, Y., and Matsuzaki, K.: Photo-Induced Formation of Peroxide in Saccharides and Related Compounds,
1238   Polymer Journal, 8, 557–563, https://doi.org/10.1295/polymj.8.557, 1976.

1239   Kumai, M.: Arctic Fog Droplet Size Distribution and Its Effect on Light Attenuation, Journal of the Atmospheric Sciences, 30,
1240   635–643, https://doi.org/10.1175/1520-0469(1973)030<0635:AFDSDA>2.0.CO;2, 1973.

1241   Lawler, M. J., Saltzman, E. S., Karlsson, L., Zieger, P., Salter, M., Baccarini, A., Schmale, J., and Leck, C.: New Insights Into the
1242   Composition and Origins of Ultrafine Aerosol in the Summertime High Arctic, Geophysical Research Letters, 48,
1243   e2021GL094395, https://doi.org/10.1029/2021GL094395, 2021.

1244   Leck, C.: Chemical composition and sources of the high Arctic aerosol relevant for cloud formation, Journal of Geophysical
1245   Research, 107, https://doi.org/10.1029/2001JD001463, 2002.

1246   Leck, C., Gao, Q., Mashayekhy Rad, F., and Nilsson, U.: Size-resolved atmospheric particulate polysaccharides in the high
1247   summer Arctic, Atmospheric Chemistry and Physics, 13, 12573–12588, https://doi.org/10.5194/acp-13-12573-2013, 2013.

1248   Lefering, I., Röttgers, R., Utschig, C., and McKee, D.: Uncertainty budgets for liquid waveguide CDOM absorption
1249   measurements, Appl. Opt., AO, 56, 6357–6366, https://doi.org/10.1364/AO.56.006357, 2017.

1250   Liu, Y., Röttgers, R., Ramírez-Pérez, M., Dinter, T., Steinmetz, F., Nöthig, E.-M., Hellmann, S., Wiegmann, S., and Bracher, A.:
1251   Underway spectrophotometry in the Fram Strait (European Arctic Ocean): a highly resolved chlorophyll a data source for
1252   complementing satellite ocean color, Opt. Express, OE, 26, A678–A696, https://doi.org/10.1364/OE.26.00A678, 2018.

1253   Macke, A. and Flores, H.: The Expeditions PS106/1 and 2 of the Research Vessel POLARSTERN to the Arctic Ocean in 2017,
1254   Bremerhaven, Germany, 171 pp., https://doi.org/10.2312/BzPM_0719_2018, 2018.

1255   Malfatti, F., Lee, C., Tinta, T., Pendergraft, M. A., Celussi, M., Zhou, Y., Sultana, C. M., Rotter, A., Axson, J. L., Collins, D. B.,
1256   Santander, M. V., Anides Morales, A. L., Aluwihare, L. I., Riemer, N., Grassian, V. H., Azam, F., and Prather, K. A.: Detection of
1257   Active Microbial Enzymes in Nascent Sea Spray Aerosol: Implications for Atmospheric Chemistry and Climate, Environ. Sci.
1258   Technol. Lett., 6, 171–177, https://doi.org/10.1021/acs.estlett.8b00699, 2019.

1259   Mari, X., Passow, U., Migon, C., Burd, A. B., and Legendre, L.: Transparent exopolymer particles: Effects on carbon cycling in
1260   the ocean, Progress in Oceanography, 151, 13–37, https://doi.org/10.1016/j.pocean.2016.11.002, 2017.

1261   Marks, R., Kruczalak, K., Jankowska, K., and Michalska, M.: Bacteria and fungi in air over the Gulf of Gdańsk and Baltic sea,
1262   Journal of Aerosol Science, 32, 237–250, https://doi.org/10.1016/S0021-8502(00)00064-1, 2001.

1263   Matsuoka, A., Bricaud, A., Benner, R., Para, J., Sempéré, R., Prieur, L., Bélanger, S., and Babin, M.: Tracing the transport of
1264   colored dissolved organic matter in water masses of the Southern Beaufort Sea: relationship with hydrographic
1265   characteristics, Biogeosciences, 9, 925–940, https://doi.org/10.5194/bg-9-925-2012, 2012.

1266 Matsuoka, A., Hooker, S. B., Bricaud, A., Gentili, B., and Babin, M.: Estimating absorption coefficients of colored dissolved
1267 organic matter (CDOM) using a semi-analytical algorithm for southern Beaufort Sea waters: application to deriving
1268 concentrations of dissolved organic carbon from space, Biogeosciences, 10, 917–927, https://doi.org/10.5194/bg-10-917-
1269 2013, 2013.

1270 Matulová, M., Husárová, S., Capek, P., Sancelme, M., and Delort, A.-M.: Biotransformation of Various Saccharides and
1271 Production of Exopolymeric Substances by Cloud-Borne Bacillus sp. 3B6, Environ. Sci. Technol., 48, 14238–14247,
1272 https://doi.org/10.1021/es501350s, 2014.

1273 May, N. W., Quinn, P. K., McNamara, S. M., and Pratt, K. A.: Multiyear study of the dependence of sea salt aerosol on wind
1274 speed and sea ice conditions in the coastal Arctic: ARCTIC SEA SALT AEROSOL, J. Geophys. Res. Atmos., 121, 9208–9219,
1275 https://doi.org/10.1002/2016JD025273, 2016.

1276 Mayol, E., Arrieta, J. M., Jiménez, M. A., Martínez-Asensio, A., Garcias-Bonet, N., Dachs, J., González-Gaya, B., Royer, S.-J.,
1277 Benítez-Barrios, V. M., Fraile-Nuez, E., and Duarte, C. M.: Long-range transport of airborne microbes over the global tropical
1278 and subtropical ocean, Nature Communications, 8, 1–9, https://doi.org/10.1038/s41467-017-00110-9, 2017.

1279 McCarthy, M., Hedges, J., and Benner, R.: Major biochemical composition of dissolved high molecular weight organic matter
1280 in seawater, Marine Chemistry, 55, 281–297, https://doi.org/10.1016/S0304-4203(96)00041-2, 1996.

1281 McCluskey, C. S., Hill, T. C. J., Humphries, R. S., Rauker, A. M., Moreau, S., Strutton, P. G., Chambers, S. D., Williams, A. G.,
1282 McRobert, I., Ward, J., Keywood, M. D., Harnwell, J., Ponsonby, W., Loh, Z. M., Krummel, P. B., Protat, A., Kreidenweis, S. M.,
1283 and DeMott, P. J.: Observations of Ice Nucleating Particles Over Southern Ocean Waters, Geophysical Research Letters, 45,
1284 11,989-11,997, https://doi.org/10.1029/2018GL079981, 2018.

1285 Mimura, T. and Romano, J. C.: Muramic Acid measurements for bacterial investigations in marine environments by high-
1286 pressure liquid chromatography, Appl. Environ. Microbiol., 50, 229–237, https://doi.org/10.1128/AEM.50.2.229-237.1985,
1287 1985.

1288 Mühlenbruch, M., Grossart, H.-P., Eigemann, F., and Voss, M.: Mini-review: Phytoplankton-derived polysaccharides in the
1289 marine environment and their interactions with heterotrophic bacteria, Environmental Microbiology, 20, 2671–2685,
1290 https://doi.org/10.1111/1462-2920.14302, 2018.

1291 Müller, K., Lehmann, S., Pinxteren, D. van, Gnauk, T., Niedermeier, N., Wiedensohler, A., and Herrmann, H.: Particle
1292 characterization at the Cape Verde atmospheric observatory during the 2007 RHaMBLe intensive, Atmospheric Chemistry
1293 and Physics, 10, 2709–2721, https://doi.org/10.5194/acp-10-2709-2010, 2010.

1294 Norris, S. J., Brooks, I. M., de Leeuw, G., Sirevaag, A., Leck, C., Brooks, B. J., Birch, C. E., and Tjernström, M.: Measurements of
1295 bubble size spectra within leads in the Arctic summer pack ice, Ocean Science, 7, 129–139, https://doi.org/10.5194/os-7-129-
1296 2011, 2011.

1297 Notz, D. and Worster, M. G.: Desalination processes of sea ice revisited, Journal of Geophysical Research: Oceans, 114,
1298 https://doi.org/10.1029/2008JC004885, 2009.

1299 Obernosterer, I., Catala, P., Lami, R., Caparros, J., Ras, J., Bricaud, A., Christine, D., Van Wambeke, F., and Lebaron, P.:
1300 Biochemical characteristics and bacterial community structure of the sea surface microlayer in the South Pacific Ocean,
1301 Biogeosciences, 5, 693–705, 2008.

1302 O'Dowd, C. D., Facchini, M. C., Cavalli, F., Ceburnis, D., Mircea, M., Decesari, S., Fuzzi, S., Yoon, Y. J., and Putaud, J.-P.:
1303 Biogenically driven organic contribution to marine aerosol, Nature, 431, 676–680, https://doi.org/10.1038/nature02959,
1304 2004.

1305 Orellana, M. V., Matrai, P. A., Leck, C., Rauschenberg, C. D., Lee, A. M., and Coz, E.: Marine microgels as a source of cloud
1306 condensation nuclei in the high Arctic, PNAS, 108, 13612–13617, https://doi.org/10.1073/pnas.1102457108, 2011.

1307 Panagiotopoulos, C. and Sempéré, R.: Analytical methods for the determination of sugars in marine samples: A historical
1308 perspective and future directions, Limnology and Oceanography: Methods, 3, 419–454,
1309 https://doi.org/10.4319/lom.2005.3.419, 2005.

1310 Papakonstantinou-Presvelou, I., Sourdeval, O., and Quaas, J.: Strong Ocean/Sea-Ice Contrasts Observed in Satellite-Derived
1311 Ice Crystal Number Concentrations in Arctic Ice Boundary-Layer Clouds, Geophysical Research Letters, 49, e2022GL098207,
1312 https://doi.org/10.1029/2022GL098207, 2022.

1313 Passow, U.: Transparent exopolymer particles (TEP) in aquatic environments, Progress in Oceanography, 55, 287–333,
1314 https://doi.org/10.1016/S0079-6611(02)00138-6, 2002.

1315 Penner, J. E., Andreae, M. O., Annegarn, H., Barrie, L., Feichter, J., Hegg, D., Jayaraman, A., Leaitch, R., Murphy, D., Nganga,
1316 J., and Pitari, G.: Aerosols, their Direct and Indirect Effects, Climate Change 2001: The Scientific Basis. Contribution of Working
1317 Group I to the Third Assessment Report of the Intergovernmental Panel on Climate Change, 289–348, 2001.

1318 Phongphattarawat, S.: Variability in pigment composition and bio-optical characteristics of phytoplankton populations in the
1319 Atlantic basin, http://purl.org/dc/dcmitype/Text, University of Oxford, 2016.

van Pinxteren, M., Müller, C., Iinuma, Y., Stolle, C., and Herrmann, H.: Chemical Characterization of Dissolved Organic Compounds from Coastal Sea Surface Microlayers (Baltic Sea, Germany), Environmental Science & Technology, 46, 10455–10462, https://doi.org/10.1021/es204492b, 2012.

van Pinxteren, M., Barthel, S., Fomba, K. W., Müller, K., Von Tümpling, W., and Herrmann, H.: The influence of environmental drivers on the enrichment of organic carbon in the sea surface microlayer and in submicron aerosol particles – measurements from the Atlantic Ocean, Elem Sci Anth, 5, https://doi.org/10.1525/elementa.225, 2017.

van Pinxteren, M., Robinson, T.-B., Zeppenfeld, S., Gong, X., Bahlmann, E., Fomba, K. W., Triesch, N., Stratmann, F., Wurl, O., Engel, A., Wex, H., and Herrmann, H.: High number concentrations of transparent exopolymer particles in ambient aerosol particles and cloud water – a case study at the tropical Atlantic Ocean, Atmospheric Chemistry and Physics, 22, 5725–5742, https://doi.org/10.5194/acp-22-5725-2022, 2022.

van Pinxteren, M., Zeppenfeld, S., Fomba, K. W., Triesch, N., Frka, S., and Herrmann, H.: Amino acids, carbohydrates, and lipids in the tropical oligotrophic Atlantic Ocean: sea-to-air transfer and atmospheric in situ formation, Atmospheric Chemistry and Physics, 23, 6571–6590, https://doi.org/10.5194/acp-23-6571-2023, 2023.

Piontek, J., Lunau, M., Händel, N., Borchard, C., Wurst, M., and Engel, A.: Acidification increases microbial polysaccharide degradation in the ocean, Biogeosciences, 7, 1615–1624, https://doi.org/10.5194/bg-7-1615-2010, 2010.

Porter, G. C. E., Adams, M. P., Brooks, I. M., Ickes, L., Karlsson, L., Leck, C., Salter, M. E., Schmale, J., Siegel, K., Sikora, S. N. F., Tarn, M. D., Vüllers, J., Wernli, H., Zieger, P., Zinke, J., and Murray, B. J.: Highly Active Ice-Nucleating Particles at the Summer North Pole, Journal of Geophysical Research: Atmospheres, 127, e2021JD036059, https://doi.org/10.1029/2021JD036059, 2022.

Prather, K. A., Bertram, T. H., Grassian, V. H., Deane, G. B., Stokes, M. D., DeMott, P. J., Aluwihare, L. I., Palenik, B. P., Azam, F., Seinfeld, J. H., Moffet, R. C., Molina, M. J., Cappa, C. D., Geiger, F. M., Roberts, G. C., Russell, L. M., Ault, A. P., Baltrusaitis, J., Collins, D. B., Corrigan, C. E., Cuadra-Rodriguez, L. A., Ebben, C. J., Forestieri, S. D., Guasco, T. L., Hersey, S. P., Kim, M. J., Lambert, W. F., Modini, R. L., Mui, W., Pedler, B. E., Ruppel, M. J., Ryder, O. S., Schoepp, N. G., Sullivan, R. C., and Zhao, D.: Bringing the ocean into the laboratory to probe the chemical complexity of sea spray aerosol, PNAS, 110, 7550–7555, https://doi.org/10.1073/pnas.1300262110, 2013.

Qin, G., Zhu, L., Chen, X., Wang, P. G., and Zhang, Y.: Structural characterization and ecological roles of a novel exopolysaccharide from the deep-sea psychrotolerant bacterium Pseudoalteromonas sp. SM9913, Microbiology, 153, 1566–1572, https://doi.org/10.1099/mic.0.2006/003327-0, 2007.

Quinn, P. K., Collins, D. B., Grassian, V. H., Prather, K. A., and Bates, T. S.: Chemistry and Related Properties of Freshly Emitted Sea Spray Aerosol, Chemical Reviews, 115, 4383–4399, https://doi.org/10.1021/cr500713g, 2015.

Rastelli, E., Corinaldesi, C., Dell'Anno, A., Lo Martire, M., Greco, S., Cristina Facchini, M., Rinaldi, M., O'Dowd, C., Ceburnis, D., and Danovaro, R.: Transfer of labile organic matter and microbes from the ocean surface to the marine aerosol: an experimental approach, Scientific Reports, 7, 1–10, https://doi.org/10.1038/s41598-017-10563-z, 2017.

Rérolle, V., Ruiz-Pino, D., Rafizadeh, M., Loucaides, S., Papadimitriou, S., Mowlem, M., and Chen, J.: Measuring pH in the Arctic Ocean: Colorimetric method or SeaFET?, Methods in Oceanography, 17, 32–49, https://doi.org/10.1016/j.mio.2016.05.006, 2016.

Robinson, T.-B., Wurl, O., Bahlmann, E., Jürgens, K., and Stolle, C.: Rising bubbles enhance the gelatinous nature of the air–sea interface, Limnology and Oceanography, 64, 2358–2372, https://doi.org/10.1002/lno.11188, 2019.

Rolph, R. J., Feltham, D. L., and Schröder, D.: Changes of the Arctic marginal ice zone during the satellite era, The Cryosphere, 14, 1971–1984, https://doi.org/10.5194/tc-14-1971-2020, 2020.

Röttgers, R., McKee, D., and Utschig, C.: Temperature and salinity correction coefficients for light absorption by water in the visible to infrared spectral region, Opt. Express, OE, 22, 25093–25108, https://doi.org/10.1364/OE.22.025093, 2014.

Röttgers, R., Doxaran, D., and Dupouy, C.: Quantitative filter technique measurements of spectral light absorption by aquatic particles using a portable integrating cavity absorption meter (QFT-ICAM), Opt. Express, OE, 24, A1–A20, https://doi.org/10.1364/OE.24.0000A1, 2016.

Russell, L. M., Hawkins, L. N., Frossard, A. A., Quinn, P. K., and Bates, T. S.: Carbohydrate-like composition of submicron atmospheric particles and their production from ocean bubble bursting, Proc. Natl. Acad. Sci. U.S.A., 107, 6652–6657, https://doi.org/10.1073/pnas.0908905107, 2010.

Šantl-Temkiv, T., Gosewinkel, U., Starnawski, P., Lever, M., and Finster, K.: Aeolian dispersal of bacteria in southwest Greenland: their sources, abundance, diversity and physiological states, FEMS Microbiol Ecol, 94, https://doi.org/10.1093/femsec/fiy031, 2018.

Šantl-Temkiv, T., Sikoparija, B., Maki, T., Carotenuto, F., Amato, P., Yao, M., Morris, C. E., Schnell, R., Jaenicke, R., Pöhlker, C., DeMott, P. J., Hill, T. C. J., and Huffman, J. A.: Bioaerosol field measurements: Challenges and perspectives in outdoor studies, Aerosol Science and Technology, 54, 520–546, https://doi.org/10.1080/02786826.2019.1676395, 2020.

Schiffer, J. M., Mael, L. E., Prather, K. A., Amaro, R. E., and Grassian, V. H.: Sea Spray Aerosol: Where Marine Biology Meets Atmospheric Chemistry, ACS Cent. Sci., 4, 1617–1623, https://doi.org/10.1021/acscentsci.8b00674, 2018.

Schill, S. R., Burrows, S. M., Hasenecz, E. S., Stone, E. A., and Bertram, T. H.: The Impact of Divalent Cations on the Enrichment of Soluble Saccharides in Primary Sea Spray Aerosol, Atmosphere, 9, 476, https://doi.org/10.3390/atmos9120476, 2018.

Schmale, J., Zieger, P., and Ekman, A. M. L.: Aerosols in current and future Arctic climate, Nature Climate Change, 11, 95–105, https://doi.org/10.1038/s41558-020-00969-5, 2021.

Schmithüsen, H.: Continuous meteorological surface measurement during POLARSTERN cruise PS106/1 (ARK-XXXI/1.1), https://doi.org/10.1594/PANGAEA.886302, 2018.

Schmithüsen, H.: Continuous meteorological surface measurement during POLARSTERN cruise PS106/2 (ARK-XXXI/1.2), https://doi.org/10.1594/PANGAEA.901179, 2019.

Schmitt-Kopplin, P., Liger-Belair, G., Koch, B. P., Flerus, R., Kattner, G., Harir, M., Kanawati, B., Lucio, M., Tziotis, D., Hertkorn, N., and Gebefügi, I.: Dissolved organic matter in sea spray: a transfer study from marine surface water to aerosols, Biogeosciences, 9, 1571–1582, 2012.

Sellegri, K., O'Dowd, C. D., Yoon, Y. J., Jennings, S. G., and Leeuw, G. de: Surfactants and submicron sea spray generation, Journal of Geophysical Research: Atmospheres, 111, https://doi.org/10.1029/2005JD006658, 2006.

Spencer, R. G. M., Aiken, G. R., Butler, K. D., Dornblaser, M. M., Striegl, R. G., and Hernes, P. J.: Utilizing chromophoric dissolved organic matter measurements to derive export and reactivity of dissolved organic carbon exported to the Arctic Ocean: A case study of the Yukon River, Alaska, Geophysical Research Letters, 36, https://doi.org/10.1029/2008GL036831, 2009.

Stedmon, C. A., Amon, R. M. W., Rinehart, A. J., and Walker, S. A.: The supply and characteristics of colored dissolved organic matter (CDOM) in the Arctic Ocean: Pan Arctic trends and differences, Marine Chemistry, 124, 108–118, https://doi.org/10.1016/j.marchem.2010.12.007, 2011.

Stein, A. F., Draxler, R. R., Rolph, G. D., Stunder, B. J. B., Cohen, M. D., and Ngan, F.: NOAA's HYSPLIT Atmospheric Transport and Dispersion Modeling System, Bull. Amer. Meteor. Soc., 96, 2059–2077, https://doi.org/10.1175/BAMS-D-14-00110.1, 2015.

Stolle, C., Nagel, K., Labrenz, M., and Jürgens, K.: Succession of the sea-surface microlayer in the coastal Baltic Sea under natural and experimentally induced low-wind conditions, Biogeosciences, 7, 2975–2988, https://doi.org/10.5194/bg-7-2975-2010, 2010.

Strong, C. and Rigor, I. G.: Arctic marginal ice zone trending wider in summer and narrower in winter, Geophysical Research Letters, 40, 4864–4868, https://doi.org/10.1002/grl.50928, 2013.

Sud, I. J. and Tyler, M. E.: Cell-Wall Composition and Osmotic Fragility of Selected Marine Bacteria, Journal of Bacteriology, 87, 696–700, 1964.

Suzuki, E. and Suzuki, R.: Variation of Storage Polysaccharides in Phototrophic Microorganisms, Journal of Applied Glycoscience, 60, 21–27, https://doi.org/10.5458/jag.jag.JAG-2012_016, 2013.

Taylor, B. B., Torrecilla, E., Bernhardt, A., Taylor, M. H., Peeken, I., Röttgers, R., Piera, J., and Bracher, A.: Bio-optical provinces in the eastern Atlantic Ocean and their biogeographical relevance, 8, 7165–7219, https://doi.org/10.5194/bgd-8-7165-2011, 2011.

Thomson, J.: Wave propagation in the marginal ice zone: connections and feedback mechanisms within the air–ice–ocean system, Philosophical Transactions of the Royal Society A: Mathematical, Physical and Engineering Sciences, 380, 20210251, https://doi.org/10.1098/rsta.2021.0251, 2022.

Triesch, N., van Pinxteren, M., Engel, A., and Herrmann, H.: Concerted measurements of free amino acids at the Cabo Verde islands: high enrichments in submicron sea spray aerosol particles and cloud droplets, Atmospheric Chemistry and Physics, 21, 163–181, https://doi.org/10.5194/acp-21-163-2021, 2021a.

Triesch, N., van Pinxteren, M., Frka, S., Stolle, C., Spranger, T., Hoffmann, E. H., Gong, X., Wex, H., Schulz-Bull, D., Gašparović, B., and Herrmann, H.: Concerted measurements of lipids in seawater and on submicrometer aerosol particles at the Cabo Verde islands: biogenic sources, selective transfer and high enrichments, Atmospheric Chemistry and Physics, 21, 4267–4283, https://doi.org/10.5194/acp-21-4267-2021, 2021b.

Triesch, N., van Pinxteren, M., Salter, M., Stolle, C., Pereira, R., Zieger, P., and Herrmann, H.: Sea Spray Aerosol Chamber Study on Selective Transfer and Enrichment of Free and Combined Amino Acids, ACS Earth Space Chem., 5, 1564–1574, https://doi.org/10.1021/acsearthspacechem.1c00080, 2021c.

Trueblood, J. V., Wang, X., Or, V. W., Alves, M. R., Santander, M. V., Prather, K. A., and Grassian, V. H.: The Old and the New: Aging of Sea Spray Aerosol and Formation of Secondary Marine Aerosol through OH Oxidation Reactions, ACS Earth Space Chem., 3, 2307–2314, https://doi.org/10.1021/acsearthspacechem.9b00087, 2019.

Tynan, E., Clarke, J. S., Humphreys, M. P., Ribas-Ribas, M., Esposito, M., Rérolle, V. M. C., Schlosser, C., Thorpe, S. E., Tyrrell, T., and Achterberg, E. P.: Physical and biogeochemical controls on the variability in surface pH and calcium carbonate saturation states in the Atlantic sectors of the Arctic and Southern Oceans, Deep Sea Research Part II: Topical Studies in Oceanography, 127, 7–27, https://doi.org/10.1016/j.dsr2.2016.01.001, 2016.

Uetake, J., Hill, T. C. J., Moore, K. A., DeMott, P. J., Protat, A., and Kreidenweis, S. M.: Airborne bacteria confirm the pristine nature of the Southern Ocean boundary layer, PNAS, 117, 13275–13282, https://doi.org/10.1073/pnas.2000134117, 2020.

Vaqué, D., Boras, J. A., Arrieta, J. M., Agustí, S., Duarte, C. M., and Sala, M. M.: Enhanced Viral Activity in the Surface Microlayer of the Arctic and Antarctic Oceans, Microorganisms, 9, 317, https://doi.org/10.3390/microorganisms9020317, 2021.

Veron, F.: Ocean Spray, Annual Review of Fluid Mechanics, 47, 507–538, https://doi.org/10.1146/annurev-fluid-010814-014651, 2015.

Walker, S. A., Amon, R. M. W., and Stedmon, C. A.: Variations in high-latitude riverine fluorescent dissolved organic matter: A comparison of large Arctic rivers, Journal of Geophysical Research: Biogeosciences, 118, 1689–1702, https://doi.org/10.1002/2013JG002320, 2013.

Wang, X., Deane, G. B., Moore, K. A., Ryder, O. S., Stokes, M. D., Beall, C. M., Collins, D. B., Santander, M. V., Burrows, S. M., Sultana, C. M., and Prather, K. A.: The role of jet and film drops in controlling the mixing state of submicron sea spray aerosol particles, PNAS, 114, 6978–6983, https://doi.org/10.1073/pnas.1702420114, 2017.

Wendisch, M., Macke, A., Ehrlich, A., Lüpkes, C., Mech, M., Chechin, D., Dethloff, K., Barientos, C., Bozem, H., Brückner, M., Clemen, H.-C., Crewell, S., Donth, T., Dupuy, R., Ebell, K., Egerer, U., Engelmann, R., Engler, C., Eppers, O., Gehrmann, M., Gong, X., Gottschalk, M., Gourbeyre, C., Griesche, H., Hartmann, J., Hartmann, M., Heinold, B., Herber, A., Herrmann, H., Heygster, G., Hoor, P., Jafariserajehlou, S., Jäkel, E., Järvinen, E., Jourdan, O., Kästner, U., Kecorius, S., Knudsen, E. M., Köllner, F., Kretzschmar, J., Lelli, L., Leroy, D., Maturilli, M., Mei, L., Mertes, S., Mioche, G., Neuber, R., Nicolaus, M., Nomokonova, T., Notholt, J., Palm, M., van Pinxteren, M., Quaas, J., Richter, P., Ruiz-Donoso, E., Schäfer, M., Schmieder, K., Schnaiter, M., Schneider, J., Schwarzenböck, A., Seifert, P., Shupe, M. D., Siebert, H., Spreen, G., Stapf, J., Stratmann, F., Vogl, T., Welti, A., Wex, H., Wiedensohler, A., Zanatta, M., and Zeppenfeld, S.: The Arctic Cloud Puzzle: Using ACLOUD/PASCAL Multi-Platform Observations to Unravel the Role of Clouds and Aerosol Particles in Arctic Amplification, Bull. Amer. Meteor. Soc., https://doi.org/10.1175/BAMS-D-18-0072.1, 2018.

Wendisch, M., Brückner, M., Crewell, S., Ehrlich, A., Notholt, J., Lüpkes, C., Macke, A., Burrows, J. P., Rinke, A., Quaas, J., Maturilli, M., Schemann, V., Shupe, M. D., Akansu, E. F., Barrientos-Velasco, C., Bärfuss, K., Blechschmidt, A.-M., Block, K., Bougoudis, I., Bozem, H., Böckmann, C., Bracher, A., Bresson, H., Bretschneider, L., Buschmann, M., Chechin, D. G., Chylik, J., Dahlke, S., Deneke, H., Dethloff, K., Donth, T., Dorn, W., Dupuy, R., Ebell, K., Egerer, U., Engelmann, R., Eppers, O., Gerdes, R., Gierens, R., Gorodetskaya, I. V., Gottschalk, M., Griesche, H., Gryanik, V. M., Handorf, D., Harm-Altstädter, B., Hartmann, J., Hartmann, M., Heinold, B., Herber, A., Herrmann, H., Heygster, G., Höschel, I., Hofmann, Z., Hölemann, J., Hünerbein, A., Jafariserajehlou, S., Jäkel, E., Jacobi, C., Janout, M., Jansen, F., Jourdan, O., Jurányi, Z., Kalesse-Los, H., Kanzow, T., Käthner, R., Kliesch, L. L., Klingebiel, M., Knudsen, E. M., Kovács, T., Körtke, W., Krampe, D., Kretzschmar, J., Kreyling, D., Kulla, B., Kunkel, D., Lampert, A., Lauer, M., Lelli, L., Lerber, A. von, Linke, O., Löhnert, U., Lonardi, M., Losa, S. N., Losch, M., Maahn, M., Mech, M., Mei, L., Mertes, S., Metzner, E., Mewes, D., Michaelis, J., Mioche, G., Moser, M., Nakoudi, K., Neggers, R., Neuber, R., Nomokonova, T., Oelker, J., Papakonstantinou-Presvelou, I., et al.: Atmospheric and Surface Processes, and Feedback Mechanisms Determining Arctic Amplification: A Review of First Results and Prospects of the (AC)3 Project, Bulletin of the American Meteorological Society, 104, E208–E242, https://doi.org/10.1175/BAMS-D-21-0218.1, 2023.

Wietz, M., Wemheuer, B., Simon, H., Giebel, H.-A., Seibt, M. A., Daniel, R., Brinkhoff, T., and Simon, M.: Bacterial community dynamics during polysaccharide degradation at contrasting sites in the Southern and Atlantic Oceans, Environ. Microbiol., 17, 3822–3831, https://doi.org/10.1111/1462-2920.12842, 2015.

Wilbourn, E. K., Thornton, D. C. O., Ott, C., Graff, J., Quinn, P. K., Bates, T. S., Betha, R., Russell, L. M., Behrenfeld, M. J., and Brooks, S. D.: Ice Nucleation by Marine Aerosols Over the North Atlantic Ocean in Late Spring, Journal of Geophysical Research: Atmospheres, 125, e2019JD030913, https://doi.org/10.1029/2019JD030913, 2020.

Williams, P. M., Carlucci, A. F., Henrichs, S. M., Van Vleet, E. S., Horrigan, S. G., Reid, F. M. H., and Robertson, K. J.: Chemical and microbiological studies of sea-surface films in the Southern Gulf of California and off the West Coast of Baja California, Marine Chemistry, 19, 17–98, https://doi.org/10.1016/0304-4203(86)90033-2, 1986.

Wurl, O., Miller, L., Röttgers, R., and Vagle, S.: The distribution and fate of surface-active substances in the sea-surface microlayer and water column, Marine Chemistry, 115, 1–9, https://doi.org/10.1016/j.marchem.2009.04.007, 2009.

Wurl, O., Miller, L., and Vagle, S.: Production and fate of transparent exopolymer particles in the ocean, Journal of Geophysical Research: Oceans, 116, https://doi.org/10.1029/2011JC007342, 2011.

Xu, M., Tsona Tchinda, N., Li, J., and Du, L.: Insoluble lipid film mediates transfer of soluble saccharides from the sea to the atmosphere: the role of hydrogen bonding, Atmospheric Chemistry and Physics, 23, 2235–2249, https://doi.org/10.5194/acp-23-2235-2023, 2023.

Xu, W., Ovadnevaite, J., Fossum, K. N., Lin, C., Huang, R.-J., Ceburnis, D., and O'Dowd, C.: Sea spray as an obscured source for marine cloud nuclei, Nat. Geosci., 15, 282–286, https://doi.org/10.1038/s41561-022-00917-2, 2022.

Yang, X., Pyle, J. A., and Cox, R. A.: Sea salt aerosol production and bromine release: Role of snow on sea ice, Geophysical Research Letters, 35, https://doi.org/10.1029/2008GL034536, 2008.

Zábori, J., Matisāns, M., Krejci, R., Nilsson, E. D., and Ström, J.: Artificial primary marine aerosol production: a laboratory study with varying water temperature, salinity, and succinic acid concentration, Atmospheric Chemistry and Physics, 12, 10709–10724, https://doi.org/10.5194/acp-12-10709-2012, 2012.

Zäncker, B., Bracher, A., Röttgers, R., and Engel, A.: Variations of the Organic Matter Composition in the Sea Surface Microlayer: A Comparison between Open Ocean, Coastal, and Upwelling Sites Off the Peruvian Coast, Frontiers in Microbiology, 8, 2369, https://doi.org/10.3389/fmicb.2017.02369, 2017.

Zäncker, B., Cunliffe, M., and Engel, A.: Eukaryotic community composition in the sea surface microlayer across an east–west transect in the Mediterranean Sea, Biogeosciences, 18, 2107–2118, https://doi.org/10.5194/bg-18-2107-2021, 2021.

Zeppenfeld, S., van Pinxteren, M., Hartmann, M., Bracher, A., Stratmann, F., and Herrmann, H.: Glucose as a Potential Chemical Marker for Ice Nucleating Activity in Arctic Seawater and Melt Pond Samples, Environ. Sci. Technol., 53, 8747–8756, https://doi.org/10.1021/acs.est.9b01469, 2019a.

Zeppenfeld, S., van Pinxteren, M., Hartmann, M., Bracher, A., Wiegmann, S., Stratmann, F., and Herrmann, H.: Glucose, T50 and salinity in the surface microlayer and bulk water samples from the Arctic during POLARSTERN cruise PS106 (2017), https://doi.org/10.1594/PANGAEA.899258, 2019b.

Zeppenfeld, S., van Pinxteren, M., Engel, A., and Herrmann, H.: A protocol for quantifying mono- and polysaccharides in seawater and related saline matrices by electro-dialysis (ED) – combined with HPAEC-PAD, Ocean Science, 16, 817–830, https://doi.org/10.5194/os-16-817-2020, 2020.

Zeppenfeld, S., van Pinxteren, M., van Pinxteren, D., Wex, H., Berdalet, E., Vaqué, D., Dall'Osto, M., and Herrmann, H.: Aerosol Marine Primary Carbohydrates and Atmospheric Transformation in the Western Antarctic Peninsula, ACS Earth Space Chem., 5, 1032–1047, https://doi.org/10.1021/acsearthspacechem.0c00351, 2021a.

Zeppenfeld, S., Fuchs, S., Rödger, S., Dietze, A., van Pinxteren, M., and Herrmann, H.: Marine carbohydrates and inorganic ions in size-resolved atmospheric particles collected over the Southern Ocean, https://doi.org/10.1594/PANGAEA.927565, 2021b.

Zeppenfeld, S., van Pinxteren, M., Fuchs, S., Hartmann, M., Gong, X., and Herrmann, H.: Inorganic ions in fog water sampled from the Arctic in 2017, https://doi.org/10.1594/PANGAEA.932573, 2021c.

Zeppenfeld, S., van Pinxteren, M., Fuchs, S., Hartmann, M., Gong, X., and Herrmann, H.: Inorganic ions in size-resolved aerosol particles sampled from the Arctic in 2017, https://doi.org/10.1594/PANGAEA.932569, 2021d.

Zeppenfeld, S., van Pinxteren, M., Fuchs, S., Hartmann, M., and Herrmann, H.: Combined carbohydrates, dissolved free carbohydrates and pH in Arctic fog water sampled during PS106, https://doi.org/10.1594/PANGAEA.962208, 2023a.

Zeppenfeld, S., van Pinxteren, M., Fuchs, S., Hartmann, M., and Herrmann, H.: Combined carbohydrates, organic carbon and total aerosol mass concentrations in size-resolved aerosol particles sampled from the Arctic in 2017, https://doi.org/10.1594/PANGAEA.962210, 2023b.

Zeppenfeld, S., Bracher, A., Wiegmann, S., Zeising, M., Fuchs, S., van Pinxteren, M., and Herrmann, H.: Dissolved and particulate combined carbohydrates, pH, inorganic ions, CDOM and particulate absorption of SML and bulk water in Arctic surface seawater and melt ponds, https://doi.org/10.1594/PANGAEA.961004, 2023c.

Zinke, J., Salter, M. E., Leck, C., Lawler, M. J., Porter, G. C. E., Adams, M. P., Brooks, I. M., Murray, B. J., and Zieger, P.: The development of a miniaturised balloon-borne cloud water sampler and its first deployment in the high Arctic, Tellus B: Chemical and Physical Meteorology, 73, 1–12, https://doi.org/10.1080/16000889.2021.1915614, 2021.